Progress in Oceanography 218 (2023) 103121

Contents lists available at ScienceDirect

Progress in Oceanography

journal homepage: www.elsevier.com/locate/pocean

Seasonality of marine calcifiers in the northern Barents Sea: Spatiotemporal distribution of planktonic foraminifers and shelled pteropods and their contribution to carbon dynamics

Griselda Anglada-Ortiz [a,*], Julie Meilland [b], Patrizia Ziveri [c,d], Melissa Chierici [e], Agneta Fransson [f], Elizabeth Jones [e], Tine L. Rasmussen [a]

[a] Department of Geosciences UiT, The Arctic University of Norway, 9037 Tromsø, Norway
[b] MARUM, Center for Marine Environmental Sciences, University of Bremen, Leobener Str. 8, 28359 Bremen, Germany
[c] Institute of Environmental Science and Technology (ICTA-UAB), Universitat Autònoma de Barcelona, 08193, Barcelona, Spain
[d] Institució Catalana de Recerca i Estudis Avançats, ICREA, 08010, Barcelona, Spain
[e] Institute of Marine Research (IMR), 9296 Tromsø, Norway
[f] Norwegian Polar Institute (NPI), 9296 Tromsø, Norway

ARTICLE INFO

Keywords:
Planktonic calcifiers
Abundances
Inorganic carbon
Organic carbon
Standing stocks
Export production

ABSTRACT

The Barents Sea is presently undergoing rapid warming and the sea-ice edge and the productive zones are retreating northward at accelerating rates. Planktonic foraminifers and shelled pteropods are ubiquitous marine calcifiers that play an important role in the carbon budget and being particularly sensitive to ocean biogeochemical changes and ocean acidification. Their distribution at high latitudes have rarely been studied, and usually only for the summer season. Here we present results of their distribution patterns in the upper 300 m in the water column (individuals m^{-3}), protein content and size distribution on a seasonal basis to estimate their inorganic and organic carbon standing stocks (μg m^{-3}) and export production (mg m^{-2} d^{-1}). The study area constitutes a latitudinal transect in the northern Barents Sea from 76° N to 82° N including seven stations through both Atlantic, Arctic, and Polar surface water regimes and the marginal and seasonal sea-ice zones. The transect was sampled in 2019 (August and December) and 2021 (March, May, and July). The highest carbon standing stocks and export production were found at the Polar seasonally sea-ice covered shelf stations with the contribution from shelled pteropods being significantly higher than planktonic foraminifers during all seasons. We recorded the highest production of foraminifers and pteropods in summer (August 2019 and July 2021) and autumn (December 2019) followed by spring (May 2021), and the lowest in winter (March 2021).

1. Introduction

The rapid increase in anthropogenic carbon dioxide (CO_2) in the atmosphere and the ocean uptake have changed and continue to change the water carbonate chemistry by reducing the pH, the carbonate ion concentration ($[CO_3^{2-}]$) and the calcium carbonate saturation state ($\Omega CaCO_3$) (Feely et al., 2004). This process, known as ocean acidification, is thought to have irreversible consequences for marine calcifiers, such as planktonic foraminifers and thecosome (shelled) pteropods. In the past the reduction of calcification rates and biogenic calcium carbonate ($CaCO_3$) production, as well as damages to (aragonitic; Ar) shells have been attributed to ocean acidification and $CaCO_3$ undersaturation ($\Omega < 1$) of the surface waters (Schiebel, 2002; Fabry, 2008; Hunt et al., 2008; Moy et al., 2009; Manno et al., 2017; Peck et al., 2018; Bednaršek et al., 2019 and references therein). However, damages to the aragonitic shell of the pteropod *Limacina helicina* have been observed even in supersaturated ($\Omega_{Ar} > 1$) conditions of $\Omega_{Ar} = 1.5$ (Bednaršek et al., 2014a; Bednaršek et al., 2019). Because of their sensitivity to $\Omega CaCO_3$, the calcareous shells of planktonic foraminifers and pteropods are considered biological indicators of ocean acidification (Orr et al., 2005; Fabry 2008; Moy et al., 2009; Bednaršek et al., 2012b). Furthermore, they have been reported to play an important role in the marine carbonate cycle and can affect the buffer capacity of the ocean by $CaCO_3$ production, export and dissolution (Schiebel, 2002; Ziveri et al., 2007; Langer, 2008; Bednaršek et al., 2012a; Buitenhuis et al., 2019; Subhas et al., 2022; Ziveri et al., 2023).

* Corresponding author.
E-mail address: Griselda.a.ortiz@uit.no (G. Anglada-Ortiz).

https://doi.org/10.1016/j.pocean.2023.103121

Available online 7 September 2023

Planktonic foraminifers are protists with a shell made of calcite and are found in all oceans, from low to high latitudes. They mainly inhabit the upper 300 m of the water column and are transported passively by ocean currents (Hemleben et al., 1989). Previous studies have reported the absence of diel vertical migration in high latitudes (Manno and Pavlov, 2013; Greco et al., 2019; Meilland et al., 2020; Ofstad et al., 2020; Anglada-Ortiz et al., 2021). When they die, their shells sink and accumulate on the seafloor and in the sediment. They preserve in the sediment when the seabed is above the calcite compensation depth (CCD) or dissolve otherwise, hereby playing an important role in the marine carbonate cycle and alkalinity budget (Schiebel, 2002; Jonkers and Kučera, 2015). Even though the seasonal distribution of living foraminifers has been studied for a long time (Allan, 1960) there is only a limited number of studies focusing on Arctic areas and the southern Barents Sea (Ofstad et al., 2020) especially outside of the summer period.

Shelled pteropods are holoplanktonic gastropods found in all oceans. Their shells are made of aragonite, a metastable form of $CaCO_3$, which is more sensitive to changes in the water carbonate chemistry than calcite (Bednaršek et al., 2012b; Manno et al., 2017). The presence of pteropod shells in the fossil record is restricted to sediments above the aragonite compensation depth, shallower than the CCD (Gerhardt and Henrich, 2001; Peijnenburg et al., 2020). However, they also play an important role in the carbonate cycle by exporting (mainly) inorganic carbon from the ocean surface (e.g. Anglada-Ortiz et al. (2021); Knecht et al. (2023); Ziveri et al. (2023)). To our knowledge, and similar to the foraminiferal fauna, the northern Barents Sea has never been studied to track the seasonality of the pteropod fauna.

The Barents Sea (Arctic Ocean) is a relatively shallow shelf sea (average water depth ~230 m) which currently experiences rapid warming, in both the atmosphere and the ocean (Dalpadado et al., 2014; Descamps et al., 2017). Coupled with a decline in sea-ice cover, the direct gas exchange with the atmosphere is predicted to increase (Bates and Mathis, 2009). The northern Barents Sea region of the Arctic is expected to be more affected by ocean acidification because of its already low carbonate saturation state (Ω) of calcite and aragonite and the higher solubility of CO_2 in cold waters (Chierici and Fransson, 2018). The study area is characterized by strong seasonal changes in light intensity and sea-ice cover. These parameters mainly drive the primary production and the availability of nutrients, together with surface stratification (Bluhm et al., 2015). Over the last few decades an increase in primary and secondary production have been observed in the Barents Sea and Arctic Ocean (Dalpadado et al., 2014; Arrigo and van Dijken, 2015; Lewis et al., 2020). In the northern Barents Sea, the primary production is characterized by a spring (phytoplankton) bloom, occurring between April and July, when the sea ice melts and retreats (Sakshaug, 1997; Lee et al., 2015). The spring bloom may be followed by a second bloom in late summer (Wassmann et al., 2019). These blooms are the most important food source for the zooplankton (Sakshaug, 1997 and references therein). Advection of Atlantic and Arctic/Polar Waters bring not only nutrients but phytoplankton and zooplankton to the northern Svalbard margin (Wassmann et al., 2019).

The marginal ice zone (MIZ) is a frontal system between Atlantic and Arctic/Polar Water (Sakshaug and Skjoldal, 1989) and characterized by high productivity and seasonality, mainly close to the sea-ice edge (Reigstad et al., 2002). This production is strongly linked to mixing of Atlantic and Arctic Water, meteorological and sea-ice conditions (Wassmann et al., 1999 and references therein). The MIZ has been expanding northwards since 1870 and accelerating since 1970 (Kinnard et al., 2008). The MIZ also affects the benthic community. A study by Saher et al. (2012) on the benthic foraminifers *Nonionellina labradorica*, a sea-ice edge indicator, showed that its distribution has been pushed northwards (100 km) as the summer sea-ice edge has moved northward during the last few decades compared to c. 40 years old data previously reported by Steinsund (1994). The seasonal ice zone (SIZ) is the transitional zone between the winter and the summer sea-ice edges (Wadhams, 1986), where the seasonally retreating and expanding sea ice generates a productive area between the open sea and the drifting pack ice (Wassmann and Reigstad, 2011).

Despite the vulnerability to ocean acidification and strong seasonality of the Northern Barents Sea, little is known about the distribution of marine calcifiers, their present state of calcification and how they would respond to ocean acidification. A recent study from the northern Svalbard margin reported that large (>500 μm) and medium-sized (250–500 μm) pteropods dominated the upper 50 m of the water column in late summer (September 2018), while medium (100–250 μm) and small-sized (<100 μm) foraminifers, dominated from 50 to 300 m at the same time (Anglada-Ortiz et al., 2021). The study also suggested that, in this region of the Arctic Ocean, pteropods compared to planktonic foraminifers contributed the most to the inorganic carbon standing stocks (66.6–96.5 %) and export production (56.7–98.4%) (Anglada-Ortiz et al., 2021). A study from the northern Barents Sea reported that adults and juveniles (>500 μm) of *L. helicina* dominated the assemblages from 0 to 300 m water depth in December 2019 during the polar night (Zamelczyk et al., 2021).

Our present study provides a seasonal quantification of carbonate contributions from foraminifers and pteropods from this remote and rarely studied Arctic region (Fig. 1). We estimate the seasonal and vertical distribution of the planktonic foraminifers and pteropods and their contribution to the inorganic and organic carbon standing stocks (μg m^{-3}) and export production (mg m^{-2} d^{-1}) over a 650 km long south-north transect from the central Barents Sea into the Arctic Ocean slope and Nansen Basin. These new data shed light on the contribution of the planktonic calcifying organisms to the carbon pump and their life cycle. This work will contribute to improve projections of environmental changes (e.g. ocean acidification) in the region and the reconstruction of past environments based on their fossil shells in sedimentary record. The sampling transect spans the Atlantic zone south of the Polar Front, over the marginal and seasonal ice zone north of the front comprising seven seasonally sampled stations.

2. Material and methods

2.1. Study area

The Barents Sea (annual mean Area = 1.47 10^6 km^2, annual mean Sea Surface Temperature = 0.9℃, annual mean Sea Surface Salinity = 34.2 (Sakshaug and Slagstad, 1991, Smedsrud et al., 2022)), is a shelf sea in the Arctic Ocean. It is influenced by both warm and relatively saline Atlantic Water flowing into the Arctic Ocean, and cold and relatively fresh Arctic Water coming in from the Arctic Ocean, this part being seasonally sea-ice covered (Sundfjord et al., 2020, Lundesgaard et al., 2022) (Fig. 1a). The Atlantic Water reaches the Barents Sea via the Norwegian Atlantic Current until it meets the southward flowing Arctic Water to form the Polar Front, where the first and southernmost station of this study is located (P1) (Fig. 1a). Environmental parameters, such as winds and currents, play an important role on mixing the water column south of the Polar Front, while north of the front a strong pycnocline between the light Polar surface Water and Atlantic Water exists during the productive season (March–October) (Sakshaug and Slagstad, 1991). North of the Polar Front, the stations P2 to P5 are influenced by the Arctic/Polar Water (Fig. 1a). These waters are created by different mixing processes, including surface cooling, sea-ice edge interactions, inflows of meltwater and Atlantic Water (Lundesgaard et al., 2022). The northernmost stations (P6 and P7), located at the northern Svalbard slope and Nansen Basin respectively, are influenced by cold Arctic/Polar Water, as well as Atlantic inflow through the West Spitsbergen Current (Fig. 1a). The strength of the Atlantic inflow varies seasonally, having its maximum during winter and minimum in summer (Vernet et al., 2019; Fer et al., 2022). Previous studies in the last decades have reported an increase in Atlantic (and warmer and more saline) inflow and an increasing abundance of subpolar organisms advected through the west

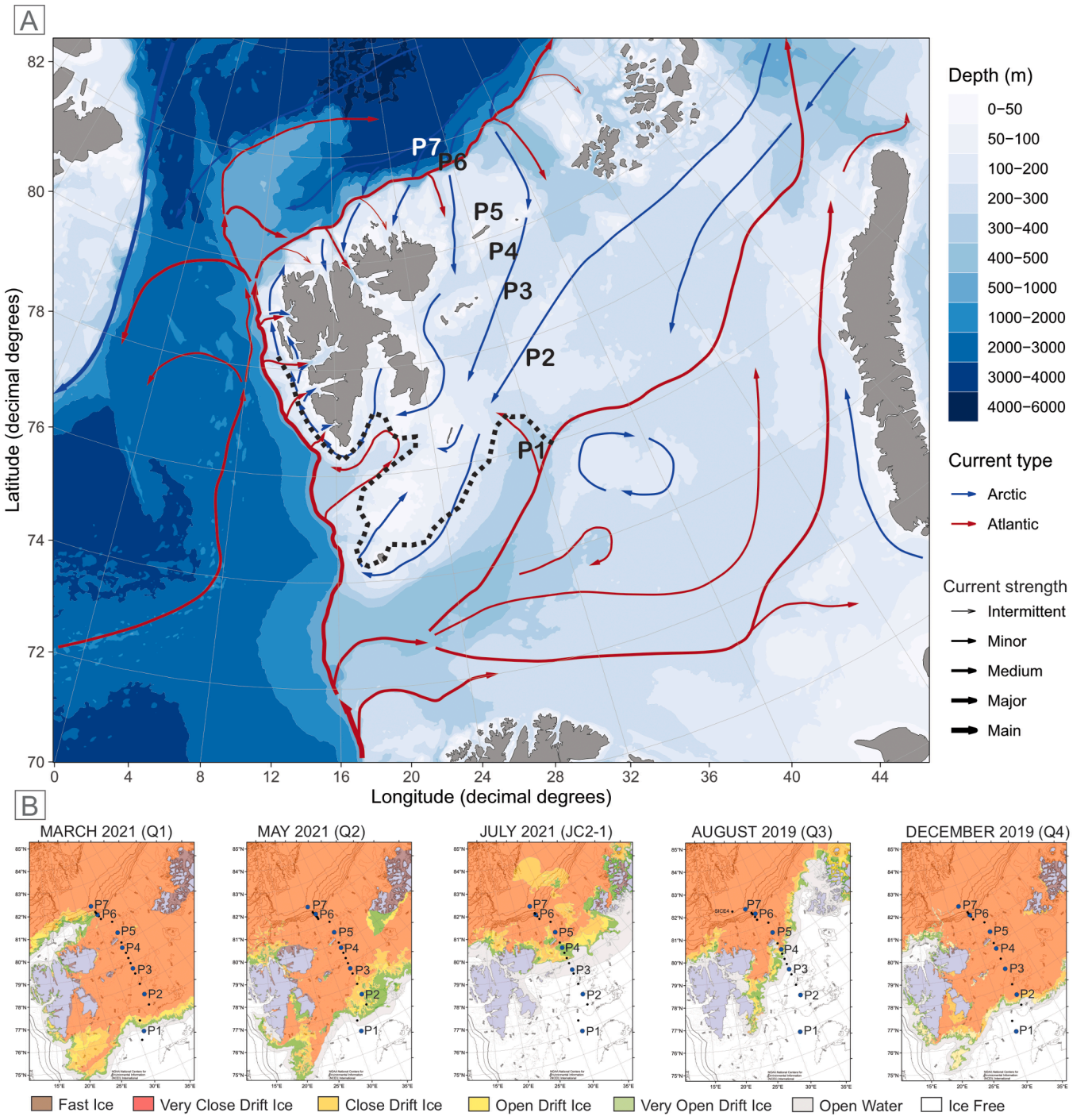

Fig. 1. (A) Location map of study area, including bathymetry and main currents (Atlantic, red arrows, and Polar ("Arctic"), blue arrows)) and strength ("current width") from R package Vihtakari (2020), and location of the Polar Front (black dashed line) from Loeng (1991). (B) Sea ice extent during the sampling months from the Norwegian Ice Service–MET Norway and bathymetry from NOAA National Centers for Environmental Information (NCEI); International Bathymetric Chart of the Arctic Ocean (IBCAO); General Bathymetric Chart of the Oceans (GEBCO).

Spitsbergen current to the northern Svalbard margin, termed "Atlantification" (Bjørklund et al., 2012; Polyakov et al., 2020; Anglada-Ortiz et al., 2021).

Station P1, south of the Polar Front, is ice-free year-round. The location of the sea ice edge changes seasonally and interannually, being at its maximum during March and at minimum during the month of September (Fetterer et al., 2017). In 2019, the sea-ice margin retreated from 75N (1st March 2019) to 80N (16th September 2019), and in 2021 from (below) 75N (1st of March 2021) to 82N (16th September 2021) (from Norwegian Meteorological Institute Ice service, 2022). The stations P2–P7 were seasonally sea-ice covered during the study period (see Fig. 1b), however the sea-ice edge in this region retreated to above 82 N in September and October 2018 (e.g. Anglada-Ortiz et al. (2021); Pieńkowski et al. (2021)). No fast ice (sea ice attached to land (Jacobs et al., 1975)) was recorded during the sampling period in the region (see Fig. 1b).

The general characteristics of the water masses present in the study area are: *Polar Water* (conservative temperature (CT) $\leq$ 0.0℃, density (σ_0) $\leq$ 27.97 kg m^{-3}), *warm Polar Water* (0.0 ℃ < CT < 4.0 ℃, absolute salinity (S_A) < 35.06 g kg^{-1}), *Atlantic Water* (CT > 2.0 ℃, $S_A \geq$ 35.06 g

kg^{-1}), and *modified Atlantic Water* (0.0 ℃ < CT ≤ 2.0 ℃, $S_A \geq 35.06$ g kg^{-1}) following the water mass classification suggested by Sundfjord et al. (2020) (Fig. 2).

2.2. Sampling and sample analyses

Plankton samples were collected onboard the RV *Kronprins Haakon* during the seasonal cruises of the Norwegian national *Nansen Legacy Project* to the Barents Sea in 2019 and 2021 (Table 1). Seven stations were sampled along a latitudinal transect east of the Svalbard archipelago (28.8°–34° E), from 76° N to 82° N covering the shelf, slope, and deep Nansen Basin, and crossing the Polar Front, the SIZ and MIZ (Fig. 1). The stations are numbered from south to north and classified as the Atlantic shelf station (south of the Polar Front) (P1), shelf stations P2–P5 (north of the Polar Front and in the MIZ), slope station (P6) and Nansen Basin station (P7) (Table 1 and Fig. 1). Data from the December cruise (absolute and relative abundance of planktonic foraminifers and pteropods) have been published in Zamelczyk et al. (2021). Data of normalized size, protein content, organic and inorganic standing stocks, and export production of the planktonic foraminifers and pteropods sampled in December 2019 are new to this study as are all other data from the other seasons in 2019 and 2021.

Samples for temperature, salinity and dissolved oxygen, nutrients (nitrite + nitrate, phosphate, silicate, $NO_2^- + NO_3^-$, PO_4^{-3} and $SiOH_4$, respectively), chlorophyll a, and carbonate chemistry were collected during all cruises and published in Reigstad (2022), Søreide (2022), Gerland (2022), Ludvigsen (2022), Jones (2022), Chierici et al. (2021a, 2021b), Jones et al. (2022a, 2022b, 2022c), Vader (2022), and Jones et al. (this issue). Ocean acidification variables (pH, calcite and aragonite saturation states, Ω_{Ca} and Ω_{Ar}, respectively) were determined from the carbonate chemistry samples following methods described in Zamelczyk et al. (2021).

Planktonic foraminifers and pteropods were collected using a midi zooplankton multinet (Hydrobios 64 μm mesh size, net opening of 50 × 50 cm = 0.25 m^2). This mesh size is the most commonly used (Manno and Pavlov 2013; Pados and Spielhagen 2014; Ofstad et al., 2020; Zamelczyk et al., 2021), together with 90 μm (Manno et al., 2012; Anglada-Ortiz et al., 2021) and 100 μm (Meilland et al., 2020) in Arctic and subarctic studies. The non-standardization of methods to collect zooplankton (e.g. by different mesh sizes of plankton nets or sediment traps), is considered to affect the quality and quantity of the collected material (Bednaršek et al., 2012a). The upper 300 m of the water column were vertically towed at regular intervals of 0–50 m, 50–100 m, 100–150 m, 150–200 m, 200–300 m in August 2019 and 0–20 m, 20–50, 50–100, 100–200, 200–300 m (200–290 m in case of P3) in March, May, and July 2021 (Table S1 (*supplementary material*)). Stations shallower than 300 m (Table 1) were sampled using the same intervals down to 170 m and 150 m in case of P2 and P5, respectively. Samples from December 2019 were collected at the intervals: 0–20 m, 20–50 m, 50–100 m, 100–200 m, 200–300 m (P1, P4, and P7); 0–20 m, 20–50 m, 50–80 m, 80–100 m, 100–170 m (P2) or 100–125 m (P5); 0–20 m, 20–50 m, 50–100 m, 100–200 m, 200–280 m (P3); and 0–20 m, 20–50 m, 50–200 m, 200–600 m, 600–750 m (P6) (Zamelczyk et al., 2021) (Table S1).

Immediately after the recovery, the samples were wet sieved though a cascade of sieves of mesh sizes 500, 250, 100 and 64 μm. Living specimens of pteropods and planktonic foraminifers from all size fractions obtained (>500 μm = large size fraction, 250–500 μm = medium size fraction, 100–250 μm = small-medium size fraction, and 63–100 μm = small fraction) were wet picked from the upper 100 m of the water column for protein extraction and measurements (see ***2.3** Organic and inorganic carbon contribution*) and frozen at −80 °C. The rest of the samples were frozen at −20 °C and were analyzed in the laboratory of the Department of Geosciences, UiT the Arctic University of Norway (Tromsø, Norway).

Each frozen sample was thawed and planktonic foraminifers containing cytoplasm and pteropod shells with the animal inside were wet picked and counted. The absolute abundance (individuals per cubic meter (ind m^{-3})) was calculated dividing the number of specimens by the volume of water sampled with the multinet. The volume of water was calculated by the equation:

$$Volume\,[m^3] = -1.2482 + (0.3298 * D\,[m])$$

with **D** being the sampled depth interval.

We classified the foraminifers by size fractions as follows: 63–100 μm as small, 100–250 μm as medium, and 250–500 μm as large. For pteropods, we have attributed each size fraction to the life stage of individuals as follows: 63–100 μm (early veliger stages), 100–250 μm (veliger or early juveniles), 250–500 μm (juveniles), and >500 μm (adults).

Based on the absolute abundances per season, station, and depth, and the average shell diameter of planktonic foraminifers and pteropods (see ***2.3** Organic and inorganic carbon contribution*), we calculated the average normalized size of a model organism of a planktonic foraminifer and a pteropod (see ***3.2** Seasonal and spatial distribution of marine calcifiers*).

2.2.1. Statistical analysis

The statistical analyses were performed using the *ggplot2* package from H (2016) from the *Rstudio* (version 4.2.1) software. To study the relation between our dataset and the environment (salinity and temperature, nutrients, chlorophyll *a*, pH, calcite and aragonite saturation states we have performed a Principal Component Analysis (PCA) and fit the distribution of planktonic foraminifers and shelled pteropods (separately) and the water masses. Moreover, we have performed a multiple linear regression and an Analysis of Variance (ANOVA) to assess the effects of environmental parameters on the abundance of foraminifers and pteropods separately, and to understand which factors best explain their distribution.

2.3. Organic and inorganic carbon contributions

The organic carbon was estimated as the individual protein content (as reported by Meilland et al. (2016) and Schiebel and Movellan (2012)) of 148 specimens of planktonic foraminifers and 300 specimens of pteropods that were individually and randomly picked from all stations and seasons onboard and were frozen at −80℃ (see ***2.2** Sampling and sample analyses*). The individual protein content is used as a proxy to estimate the organic carbon content of the organism, where 1 mg of protein equals to 1 mg of organic carbon. We followed the BCA (bicinchoninic acid) protocol from Meilland et al. (2016) using the nanospectrophotometer (NanoDrop 2000®) at the Department of Arctic and Marine Biology, UiT the Arctic University of Norway (Tromsø, Norway). This technique does not affect their aragonitic and calcitic shells, allowing us to use them for further analyses, e.g. size measurements (diameter and mass) or scanning electron microscopy (SEM).

The mass of solid inorganic carbon ($CaCO_3$) of planktonic foraminifers and pteropods was estimated by measuring the shell diameter of the specimens analyzed for protein content, applying the equations previously reported for foraminifers ($y_w = 2.04*10^{05}x^{2.2}$ from Meilland et al. (2018)) and pteropods (for *L. helicina)* ($DW = 0.137*D^{1.5055}$ from Bednaršek et al. (2012a)) separately. The 148 planktonic foraminifers (*48* specimens from 63 to 100 μm; *92* from 100 to 250 μm; and *8* from 250 to 500 μm) and 300 pteropods (*24* from the 63–100 μm size fraction; *67* from 100 to 250 μm; *59* from 250 to 500 μm; and *150* > 500 μm) were photographed with a DMC4500 camera attached to a Leica Z16 APO binocular (magnification × 0.57–9.2). We measured their diameter (pteropods) and minimum diameter (foraminifers) (see Fig. S1) using the ImageJ software (Schneider et al., 2012).

The carbon standing stocks (μg m^{-3}) of foraminifers and pteropods have been estimated by extrapolating their protein content and shell diameter, for the organic or inorganic contribution, respectively (see ***3.3***

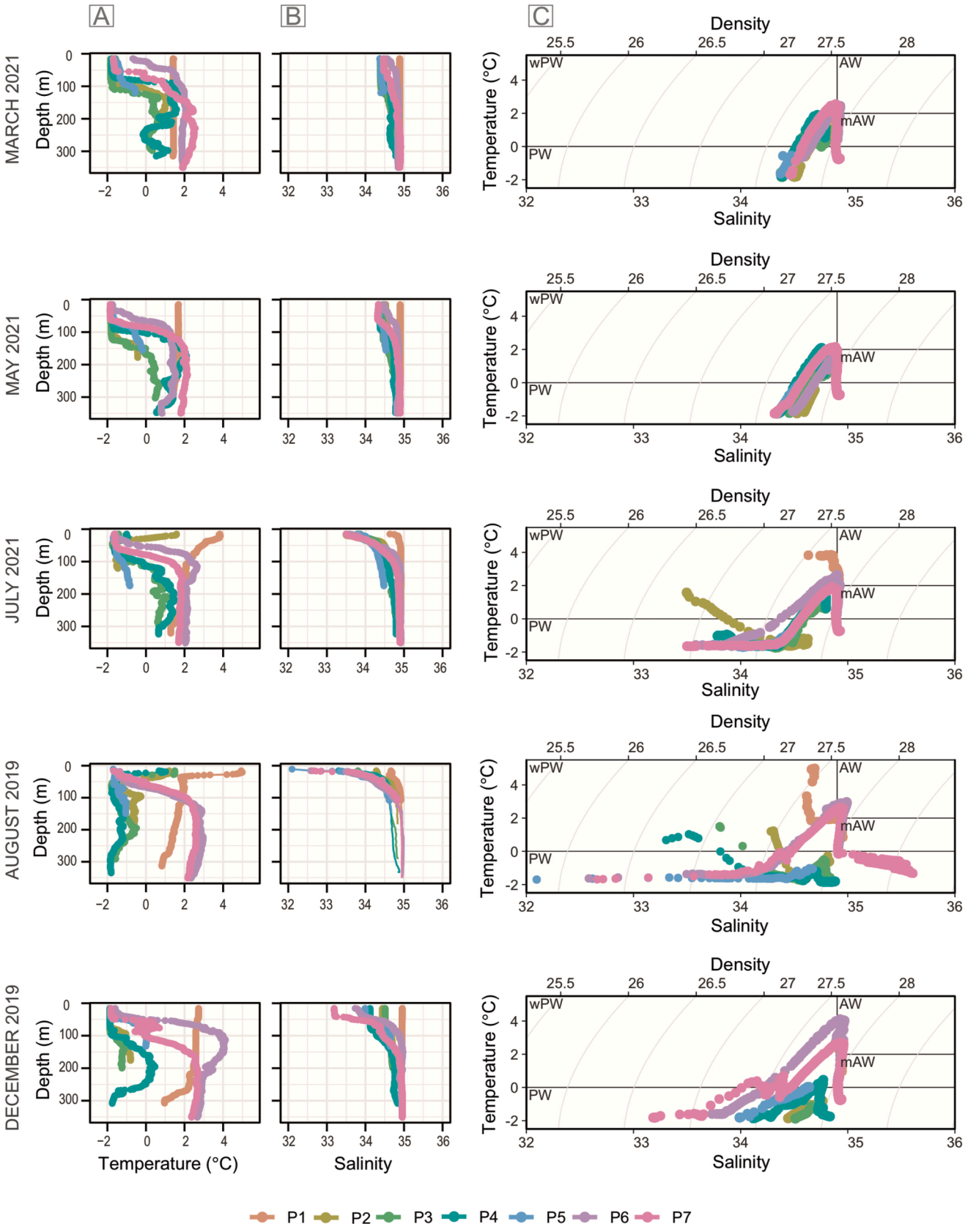

Fig. 2. Vertical temperature (A) and salinity (B) of the transect from the different seasons. Temperature-Salinity (T-S) profile (C) with water mass classification from Sundfjord et al., 2020: Polar Water (PW), warm Polar Water (wPW), Atlantic Water (AW), and modified Atlantic Water (mAW).

Table 1
Location, latitude, longitude, water depth, multinet sampling intervals (August, March, May, and July) and multinet sampling dates from each cruise (Q3 = August 2019, Q4 = December 2019, Q1 = March 2021, Q2 = May 2021, JC2-1 = July 2021).

	Location	Latitude (N)	Longitude (E)	Water depth (m)	Sampling interval(m)	Date (Q3)	Date (Q4)	Date (Q1)	Date (Q2)	Date (JC2-1)
P1	Shelf	76	31.22	322	0–300	08.08.2019	12.12.2019	05.03.2021	30.04.2021	14.07.2021
P2	Shelf	77.5	34	190	0–170	12.08.2019	10.12.2019	07.03.2021	02.05.2021	15.07.2021
P3	Shelf	78.7	34	307	0–300	–	09.12.2019	08.03.2021	03.05.2021	17.07.2021
P4	Shelf	79.7	34.23	332	0–300	14.08.2019	08.12.2019	09.03.2021	05.05.2021	18.07.2021
P5	Shelf	80.5	33.96	158	0–150	16.08.2019	06.12.2019	12.03.2021	07.05.2021	19.07.2021
P6	Slope	81.5	31.5	840	0–300	18.08.2019	05.12.2019	16.03.2021	10.05.2021	22.07.2021
P7	Basin	82	28.8	3120	0–300	21.08.2019	02.12.2019	17.03.2021	14.05.2021	24.07.2021

Organic and inorganic carbon of marine calcifiers) and integrating their absolute abundances from the upper 100 m of the water column following the published literature (Schiebel and Hemleben, 2000; Schiebel, 2002; Bednaršek et al., 2012a; Meilland et al., 2016; Anglada-Ortiz et al., 2021). Similarly, the export productions (mg m^{-2} d^{-1}) have been estimated using protein content and shell diameter, their abundances between 50 and 100 m (or 80–100 m), except for station P6 in December, which was 200 m, and their test sink velocity (Schiebel and Hemleben, 2000; Schiebel, 2002; Bednaršek et al., 2012a; Meilland et al., 2016; Anglada-Ortiz et al., 2021).

3. Results

3.1. Environmental properties of water masses

In summer (August and July) and late autumn (December) we observed a wider range in temperatures and salinities, associated with the higher atmospheric temperatures and melting of sea ice, compared to winter (March) and spring (May) (Fig. 2a, 2b). In terms of temperature, the slope station (P6) and basin station (P7) (ice covered during all cruises, see Fig. 1b) varied less along the seasons than the other stations (see Fig. 2a). Moreover, we observed lower surface salinities in July, August, and December (Fig. 2b). The stations P5, P6 and P7 were associated with very closed drift ice during all sampling seasons, while stations P2 and P4 were associated with variable sea ice conditions, consisting of very open drift ice, open drift ice, and very close drift ice in August, July and May, respectively (Fig. 1b). In all seasons, the surface water (20–50 m) consisted of Atlantic and modified Atlantic Water at the stations P1, P6 and P7, while the other stations (P2–P5) were characterized by Polar Water and warm Polar Waters (Fig. 2c).

3.2. Seasonal and spatial distribution of marine calcifiers

A clear seasonal pattern of temporal and spatial distribution of the studied planktonic calcifiers has been identified. The overall highest seasonal absolute abundances of living planktonic foraminifers and pteropods (ind m^{-3}) were observed in August 2019, followed by July

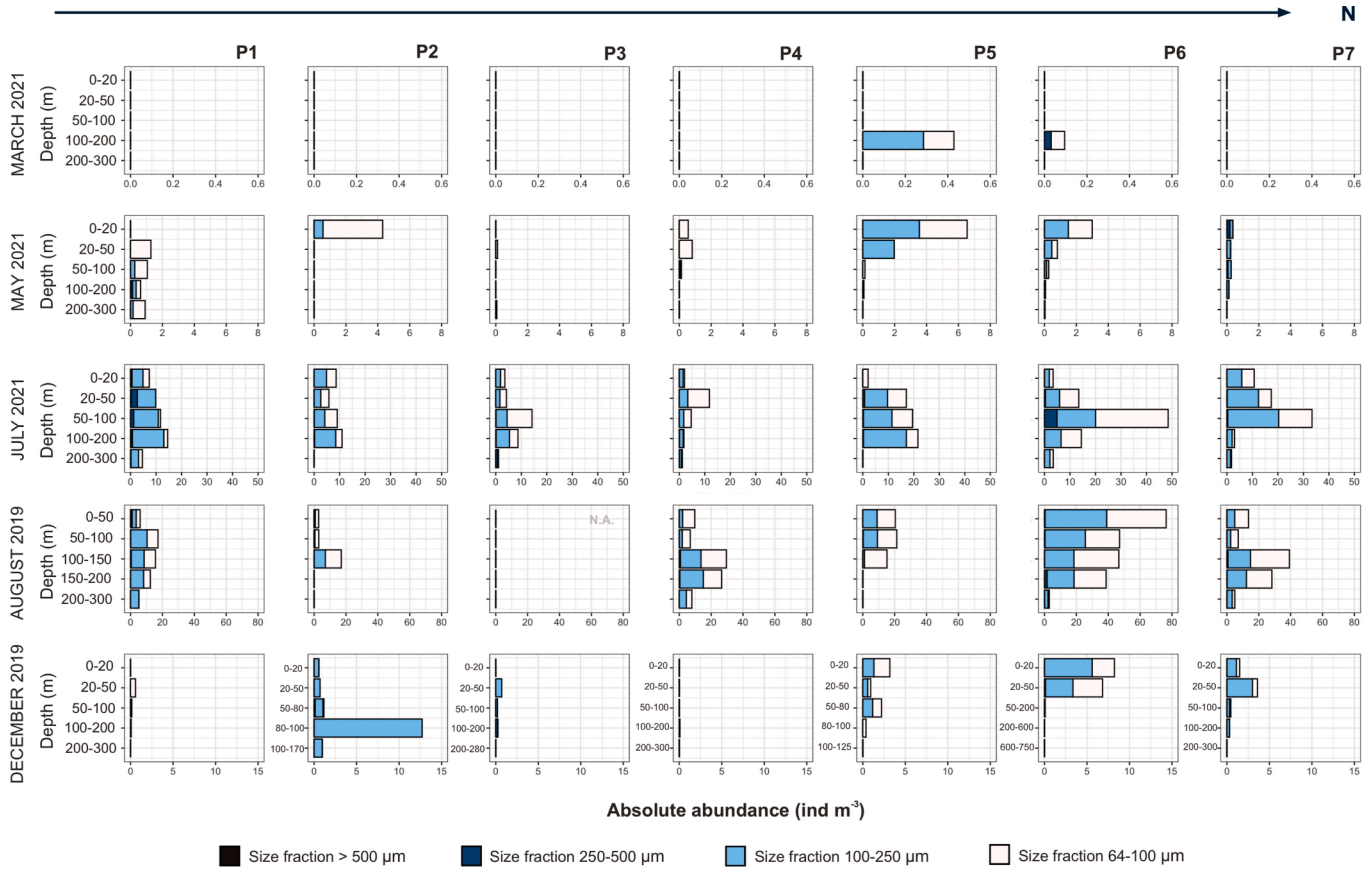

Fig. 3. Absolute abundances (ind m^{-3}) of planktonic foraminifers containing cytoplasm in the various size fractions (note change in x-axis) along P stations (columns) and seasons (rows). December data from Zamelczyk et al. (2021) (note different y-axes).

2021 and May 2021, with the lowest in March 2021 (Figs. 3, 4 and 9). Regarding the vertical distribution of marine calcifiers and their group relative abundance (planktonic foraminifers vs pteropods) and the environmental conditions, from now on we will refer to the stations with the following categories: shelf station south of the Polar Front (Atlantic station P1), shelf stations north of the Polar Front (Polar stations P2–P5), slope station (P6), and basin station (P7). The environmental parameters seem to follow a depth distribution, and in general the abundance of shelled pteropods is the highest when the temperature is low (Fig. S2).

In March, the highest abundances (22 ind m^{-3}) of calcifiers were found at P2 at depth (100 –200 m), while the lowest (0 ind m^{-3}) at P1 throughout the water column (0–20, 20–50, 50–100, and 100–200 m), P2 at the surface and subsurface (0–20, 20–50, and 50–100 m), and P3 at the surface (0–20 m) (Figs. 3 and 4). Foraminifers were only present at stations P5 and P6 at depth (100–200 m) in very low abundances (0.4 and 0.1 ind m^{-3}, respectively), while pteropods completely dominated the assemblages (av 99%, min 87%, max 100%) (Figs. 3, 4 and 9a). The foraminiferal community was dominated by medium sized organisms, while the pteropod community was dominated by small veliger larvae (Figs. 3 and 4) (see *supplementary material* for details).

In May, the highest abundance (50 ind m^{-3}) of calcifiers occurred at P2 at subsurface (50–100 m). In this season we observed an increasing presence of planktonic foraminifers (av 30%) when compared to March and to pteropods (av 70%) (Figs. 3 and 9a). The basin station was the only one dominated by planktonic foraminifers, while pteropods dominated the upper 300 m of the water column at the Polar stations and represented (approximately) half of both groups at the Atlantic and slope stations, (Fig. 9a) (see *supplementary material* for details). The foraminiferal community was dominated by small-medium sized organisms, while the pteropod community was dominated by veliger/young juveniles (Figs. 3 and 4).

In July, the highest abundance (60 ind m^{-3}) of calcifiers was found at P3 at subsurface (20–50 m), and the lowest (1 ind m^{-3}) at depth (200–300 m) (Figs. 3 and 4). Foraminifers dominated the assemblages (av 74%), while pteropods were less abundant at depth and at the northernmost stations (av 26%) (Figs. 3, 4 and 9a). In general foraminifers dominated throughout the upper water column at the Atlantic station, slope, and basin stations, while pteropods dominated the Polar stations, except at P5 (Fig. 9a) (see *supplementary material* for details). The planktonic foraminiferal community was dominated by small and small-medium specimens, while pteropods by juveniles/young adults (Figs. 3 and 4).

In August the highest (82 ind m^{-3}) abundances of calcifiers were found at station P5 at depth (100–150 m) and the lowest (4 ind m^{-3}) at stations P6 at depth (200–300 m) (Figs. 3 and 4). Opposite to the other stations, where high abundances were found at the surface (0–50 m) and decreasing with depth, the abundances at P5 (mainly pteropods) increase at depth (100–150 m) (Fig. 4). Almost no pteropods were collected from the slope (P6) and basin (P7) stations in this (or any) season (Fig. 4). In general, foraminifers dominated the upper 300 m of the water column at the Atlantic station, slope, and basin stations, while pteropods at the Polar stations, with exception of P4 (Fig. 9a, 9b). The planktonic foraminiferal community was dominated by small and small-medium specimens, while pteropods by juveniles/young adults (Figs. 3 and 4) (see *supplementary material* for more details).

In December, the highest abundance (43 ind m^{-3}) of calcifiers was found at P5 at surface (0–50 m), while the lowest (<0.04 ind m^{-3}) at P1, P6, and P7 all at depth below 200 m (Figs. 3 and 4). On average, the abundance of pteropods (57%) was higher than the foraminifers along the transect and they dominated the assemblage in the Polar stations (av 82%, min 0%, max 100%) (Figs. 3, 4 and 9a, 9b). The foraminiferal community was dominated by medium and small-medium specimens,

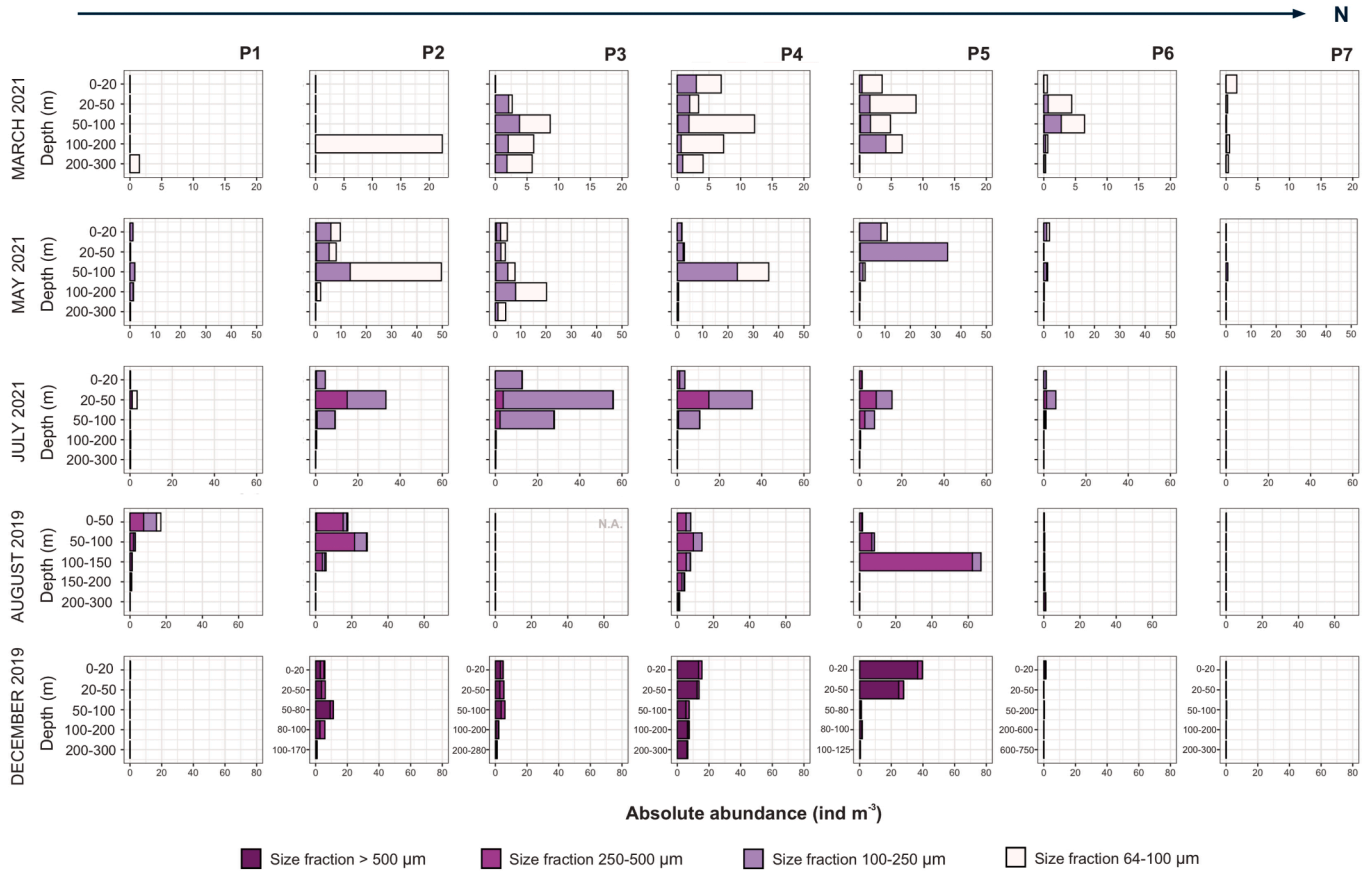

Fig. 4. Absolute abundances (ind m^{-3}) of pteropod shells containing the animal in the various size fractions (note change in x-axis) along P stations (columns) and seasons (rows). December data from Zamelczyk et al.(2021) (note different y-axes).

while the pteropods by adults (see Figs. 3, 4 and Zamelczyk et al. (2021)).

3.3. Organic and inorganic carbon of marine calcifiers

3.3.1. Protein content of foraminifers and pteropods

The protein content of 148 and 300 living foraminifers and pteropods, respectively, was correlated to the length of the organisms, being directly proportional for foraminifers and logarithmic for pteropods (Fig. 5). The protein-length of pteropods was better correlated than in the case of planktonic foraminifers (R^2 = 0.68 and R^2 = 0.2, respectively) (Fig. 5). The protein content of foraminifers, as well as their size, were significantly smaller in terms of values and variability compared to pteropods (Fig. 5).

3.3.2. Seasonal variability of planktonic foraminifers and pteropod size distribution

The normalized size of calcifiers based on their abundance, changed along the seasons. For both planktonic foraminifers and pteropods, we observed larger average sizes in December 2019, followed by August 2019, July 2021, and May 2021, and the lowest, in March 2021 (Fig. 6). The size range of foraminifers from 0 to 300 m and the upper 100 m was widest in December 2019 and May 2021 (Fig. 6a, 6b), and in the case of pteropods, in August and December 2019 and May 2021 (Fig. 6d, 6e). Below 100 m water depth, the highest size range of foraminifers was in March 2021 (Fig. 6g) and for pteropods, December 2019 (Fig. 6f). We did not observe larger organisms below 100 m that could suggest ontogenic vertical migration.

3.4. Seasonal and spatial variability in carbon dynamics

3.4.1. Carbon standing stock in the upper 0–100 m water depth [μg m^{-3}]

We have recorded the highest carbon standing stocks of both pteropods and foraminifers combined in December 2019 (av 458 ± 520 μg m^{-3}; min 3 μg m^{-3}; max 1401 μg m^{-3}), followed by August 2019 (av 269 ± 368 μg m^{-3}; min 7 μg m^{-3}; max 1002 μg m^{-3}), July 2021 (av 79 ± 75 μg m^{-3}; min 21 μg m^{-3}; max 233 μg m^{-3}), and May 2021 (av 52 ± 51 μg m^{-3}; min 3 μg m^{-3}; max 113 μg m^{-3}), and the lowest in March 2021 (av 12 ± 12 μg m^{-3}; min 0 μg m^{-3}; max 29 μg m^{-3}) (Fig. 7a and Table S2). The highest carbon standing stocks were found along the polar stations (P2 in August and May, P5 in December, P4 in March, and P3 in July), and lowest at the Atlantic, slope and basin stations (P1 in December and March, and P7 in August, May, and July) (Fig. 7b, Table S2). On average, the organic contribution to the total carbon of each group is different, because pteropods are larger (av 15%) than foraminifers (av 0.1%). In all seasons, pteropods dominate the total (both organic and inorganic) carbon standing stocks of the planktonic calcifiers (av 50%), recording their highest contribution at the shelf stations (av c. 70–100%) (Table S2) (see also *supplementary material* for more details).

3.4.2. Carbon export production at 100 m water depth [mg m^{-2} d^{-1}]

We recorded the highest carbon export production of foraminifers and pteropods together in August 2019 (av 149 ± 249 mg m^{-2} d^{-1}; min 0.4 mg m^{-2} d^{-1}; max 647 mg m^{-2} d^{-1}), followed by December 2019 (av 76 ± 93 mg m^{-2} d^{-1}; min 0.02 μg m^{-3}; max 232 mg m^{-2} d^{-1}), July 2021 (av 32 ± 31 mg m^{-2} d^{-1}; min 5 mg m^{-2} d^{-1}; max 95 mg m^{-2} d^{-1}), and May 2021 (av 29 ± 38 mg m^{-2} d^{-1}; min 0.9 mg m^{-2} d^{-1}; max 77 mg m^{-2} d^{-1}), and the lowest in March 2021 (av 8 ± 8 mg m^{-2} d^{-1}; min 0 mg m^{-2} d^{-1}; max 17 mg m^{-2} d^{-1}) (Fig. 8a). The highest carbon export production was found along the polar stations (P2 in August, P3 in March and July, and P4 in December and May), while the lowest at the Atlantic, slope and basin stations (P1 in December and March, P6 in May, and P7 in August and July) (Fig. 8b). The organic contribution of pteropods was larger (av 14%) than foraminifers (av 0.07%). In all seasons, pteropods drove the total (organic and inorganic) carbon export production (av >66%), recording their highest contribution along the shelf stations (c. 75–100%). In general, the export production followed the same trend as

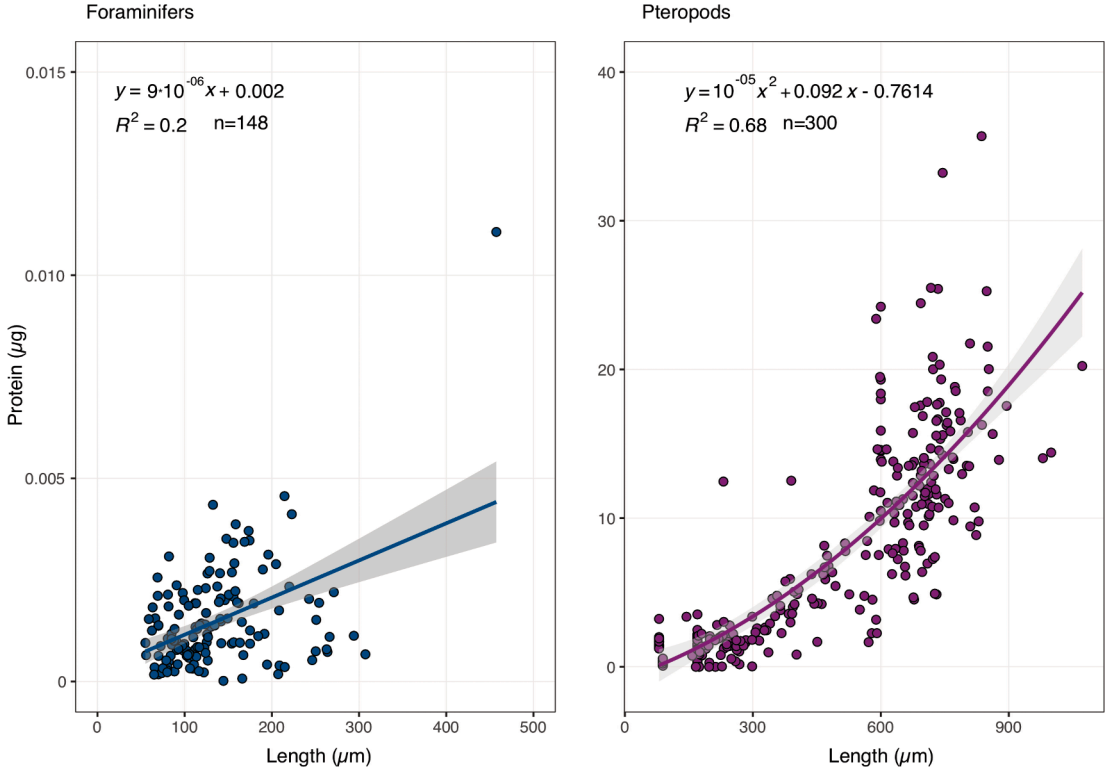

Fig. 5. Protein content (μg) of foraminifers (left) and pteropods (right) relative to shell length (μm) with the equations used to estimate organic content (see 2.3 Organic and inorganic carbon contribution). Note different scales on the x- and y-axis.

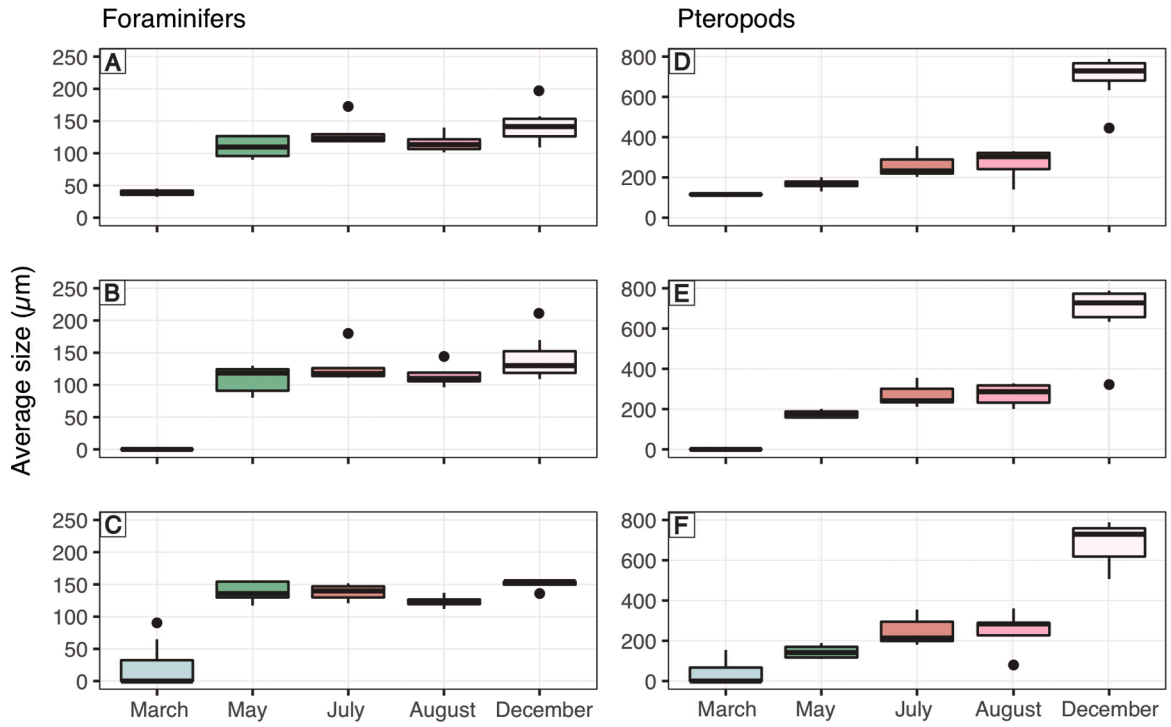

Fig. 6. Average size (μm) of foraminifers (integrating 0–300 m (A), 0–100 m (B), and below 100 m (C)) and pteropods (integrating 0–300 m (D), 0–100 m (E), and below 100 m (F) for each season. The black dots are outliers from the seasonal measurements. Note different scales on the y-axes.

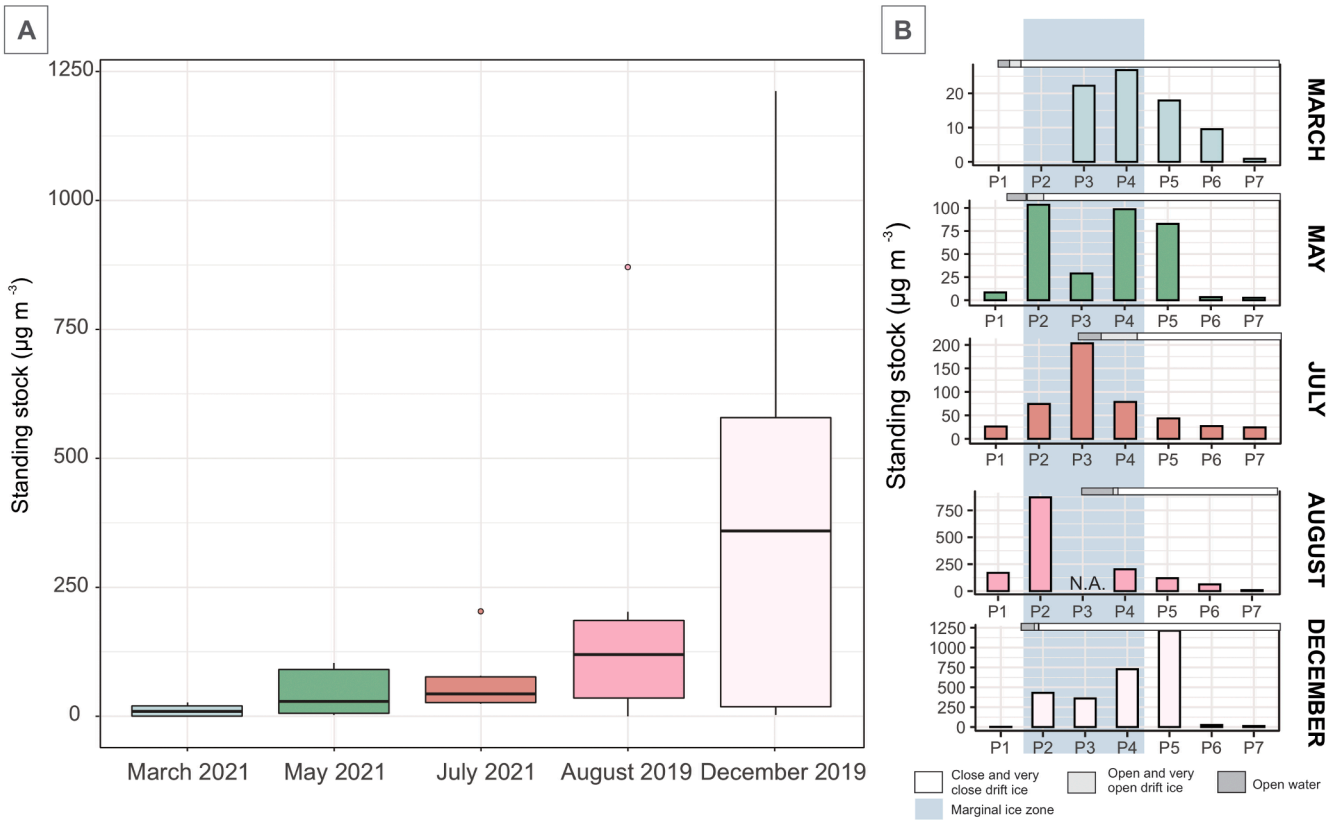

Fig. 7. Panel A: Total carbon (organic and inorganic) standing stocks (from 0 to 100 m depth, μg m^{-3}) from planktonic foraminifers and shelled pteropods in five different seasons, each of them represented by a different color (August 2019: pink; December 2019: light pink; March 2021: light blue; May 2021: green; and July 2021: orange). Panel B: Detailed standing stocks at each station during the different seasons and information about sea ice cover (close and very close drift ice: white; open and very open drift ice: light grey; open water: grey) and seasonal ice zone (blue) (note different y-axes at panel B).

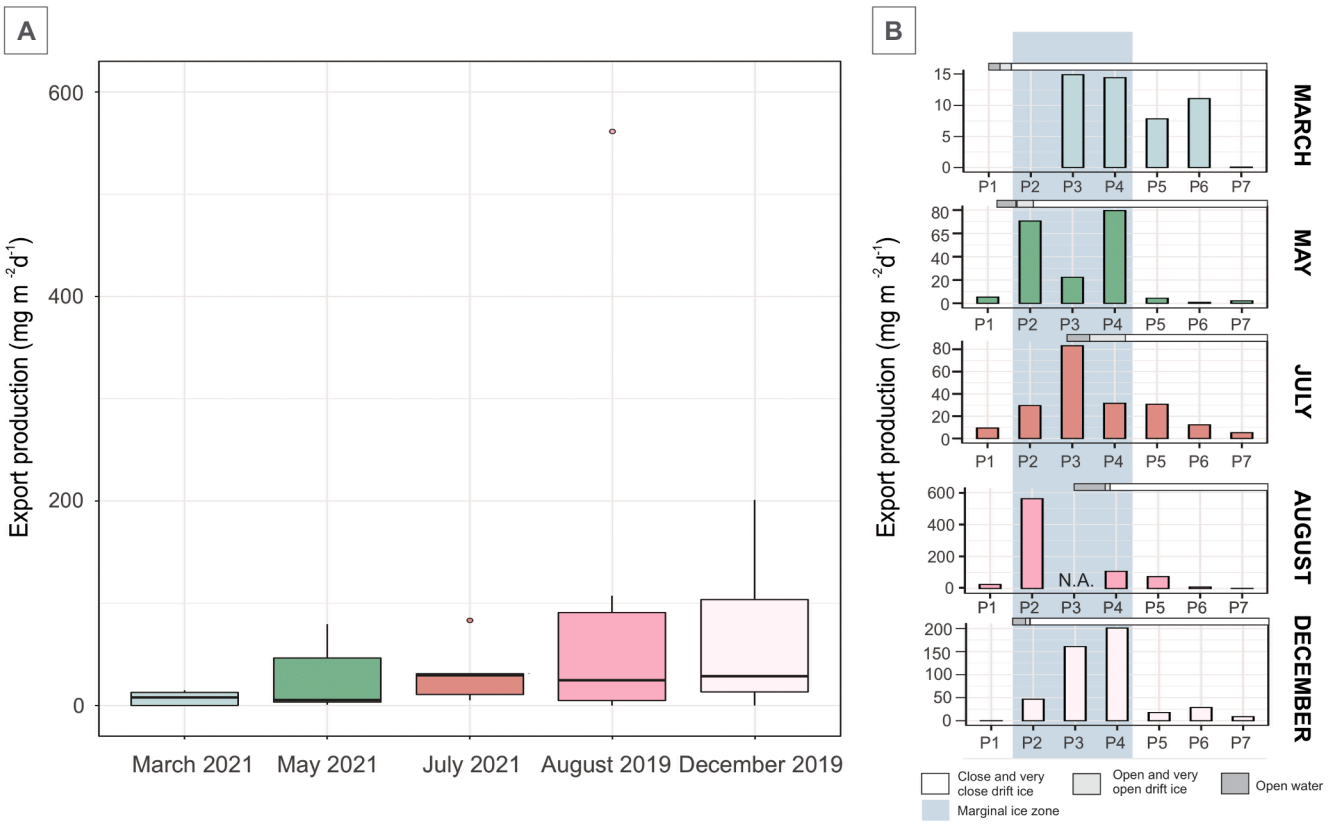

Fig. 8. Panel A: Total carbon (organic and inorganic) export production (at 100 m depth, mg $m^{-2}d^{-1}$) from planktonic foraminifers and shelled pteropods in five different seasons, each of them represented by a different color (August 2019: pink; December 2019: light pink; March 2021: light blue; May 2021: green; and July 2021: orange). Panel B: Detailed export production at each station during the different seasons and information about sea ice cover (close and very close drift ice: white; open and very open drift ice: light grey; open water: grey) and seasonal ice zone (blue) (note different y-axes at panel B).

the carbon standing stocks (Figs. 7 and 8). The values that differ the most were found at P5 in December (Figs. 7 and 8), with high abundances of pteropods (young adults) at the surface (0–50 m) (Fig. 4) (see also *supplementary material* for more details).

4. Discussion

In this study we have observed the highest abundance of planktonic foraminifers and pteropods in August and July, followed by December and May, and with a minimum in March. However, the largest diameter of calcifiers and the associated total carbon standing stock and export production were estimated for December, followed by August and July, May, and March. We find the highest production of foraminifers in summer in the Atlantic zones south of the Polar front and in the Arctic Ocean in the northern part of the MIZ (P1, P6 and P7; Fig. 3). For pteropods production is highest in the polar stations and along the MIZ and SIZ during most seasons (P2–P5; Fig. 4).

4.1. Pattern in abundance, seasonality and water masses

Due to difficulties of sampling and accessibility in the Arctic region, most studies have been carried out during the summer season. From all Arctic regions, planktonic foraminifers have been mostly studied in the Fram Strait (e.g. Carstens et al., 1997; Volkmann, 2000; Stangeew, 2001; Manno and Pavlov, 2013; Pados and Spielhagen, 2014; Greco et al., 2022). Here, the abundances of living planktonic foraminifers are 30–60 ind m^{-3} in June-July-early August (Volkmann, 2000; Manno and Pavlov, 2013; Pados and Spielhagen, 2014), while the mean abundance of foraminifers in the Arctic Basin was 25.4 ind m^{-3} (Tell et al., 2022). Carstens et al. (1997) reported different maxima in abundances along the Fram Strait in August of 1250 ind m^{-3} and 100 ind m^{-3} at 78° and 80°N, respectively. The abundances in the Barents Sea (6–12 ind m^{-3}) (Volkmann, 2000), are comparable to the current study (5–15 ind m^{-3}, and 10–35 ind m^{-3} in July and August, respectively). Ofstad et al. (2020) reported abundances in the southern Barents Sea in April (0–6 ind m^{-3}) comparable to May in the current study; while the highest were found in June (436 ind m^{-3}) and exceeding any of the abundances found in the summer months in the northern Barents Sea (Fig. 3). The higher values compared to this study could be attributed to a higher productivity in the southern Barents Sea compared to the northern part and/or influence of strong seepage of methane probably causing upwelling (Ofstad et al., 2020). The abundances found along the north Svalbard margin in September (2.3–52.6 ind m^{-3}, Anglada-Ortiz et al., 2021) agrees with the values found in the northern Barents Sea in July and August (Fig. 3).

In general for pteropods, lower abundances were reported compared to the present study in the southern Barents Sea (Ofstad et al., 2020) and the northern Svalbard margin (Anglada-Ortiz et al., 2021), probably related to local differences in water masses and presence/absence of sea ice. Abundances from the Atlantic shelf station (P1) from August and July are comparable to the results from the southern Barents Sea in June and April, respectively (Ofstad et al., 2020).

The stations P1 (south of the SIZ), and P6–P7 (north of the SIZ) have generally the lowest (total) abundances in all seasons. Planktonic foraminifers are more abundant in the Atlantic influenced stations (P1, P6 and P7), while pteropods are more abundant in the Arctic productive stations P2–P5 (Figs. 9 and S3). The distribution of planktonic foraminifers observed in the current study is associated with temperature, with higher abundances in warmer waters (Atlantic influenced stations P1, P6 and P7) (Figs. 3, S2 and S3). Their vertical distribution does not follow a specific depth pattern, but it changes through seasons (Fig. 3). In spring and winter, their highest abundances are found at the upper

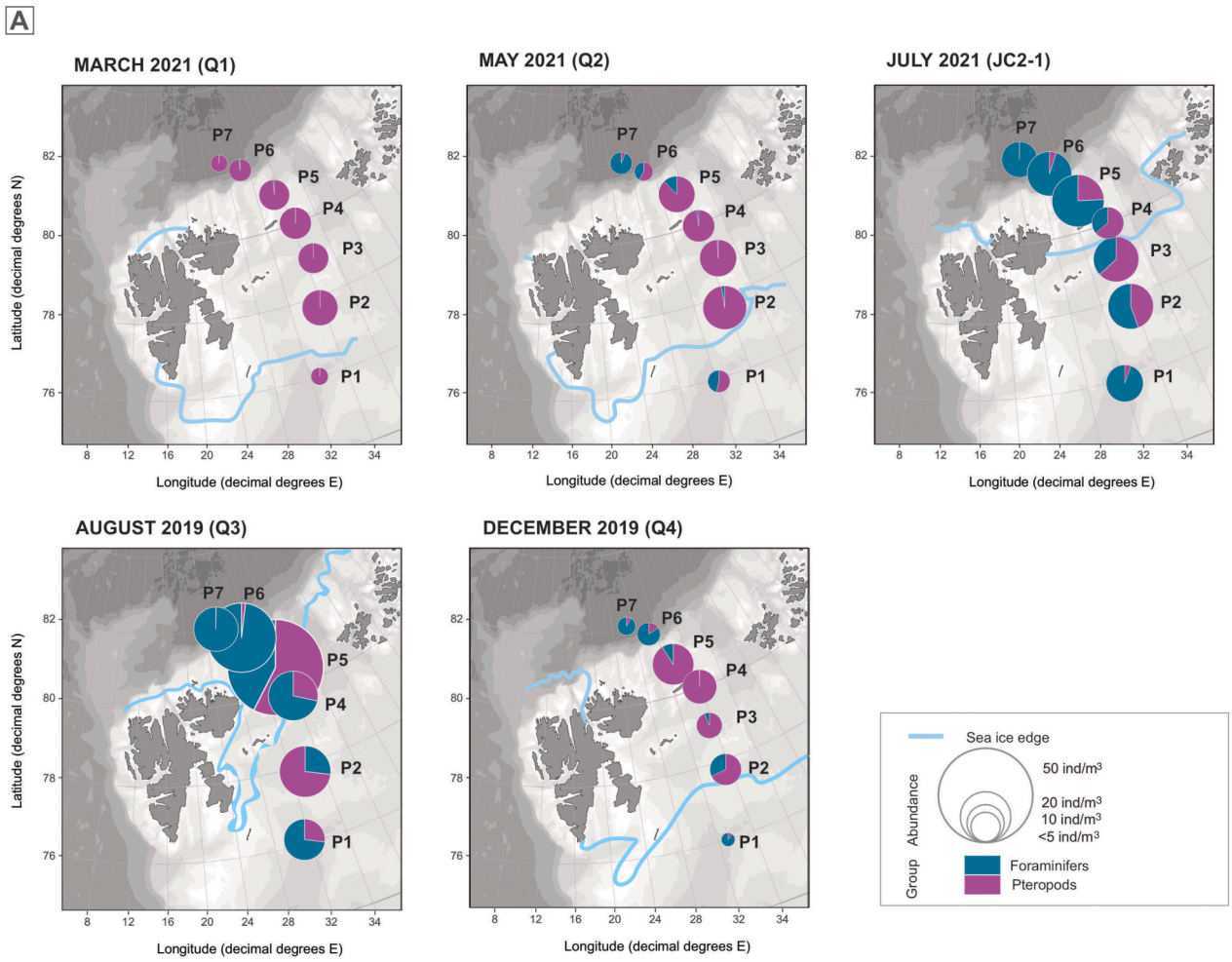

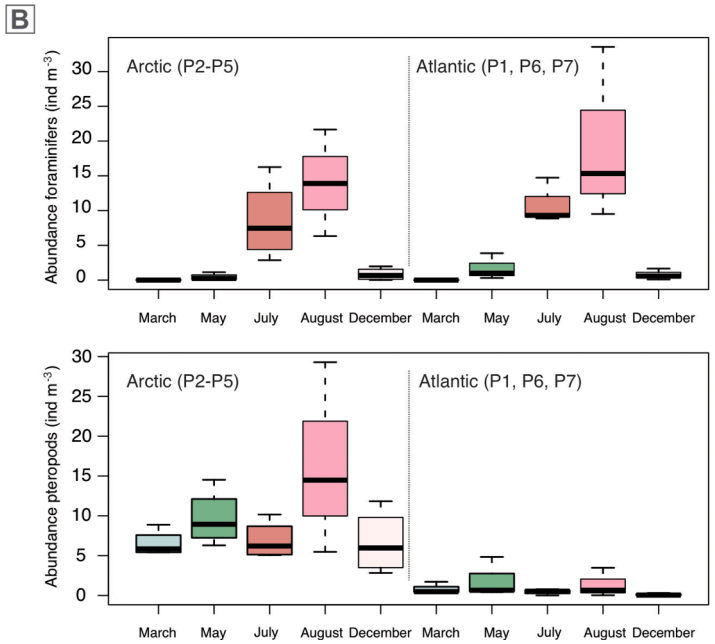

	p value
Abundance/season	0.223
Abundance/water mass	0.408
Season/Water mass	0.817

	p value
Abundance/season	0.868
Abundance/water mass	0.0000302 ***
Season/Water mass	0.612

Fig. 9. Panel A: Depth integrated abundance (ind m^{-3}) of all size fractions of planktonic foraminifers (dark blue) and shelled pteropods (purple) from the upper 300 m of the water column (with exception of station P6 in December, which only considers the upper 200 m), and sea-ice edge from the Norwegian Ice Service–MET Norway (in light blue). The size of the circles represents the total absolute abundance. Panel B: Distribution and results of the two-way ANOVA test of planktic foraminifers (upper panels) and pteropods (lower panels) in the Arctic (P2 – P5) and Atlantic (P1, P6 and P7) influenced stations during all seasons. ***$p < 0.01$.

50–100 m of the water column, while in summer they are spread throughout the water column (Fig. 3) and potentially following the distribution of food. Their abundances and distribution are significantly explained ($p < 0.05$) by the temperature and nutrients (NO_2^-, NO_3^- and $SiOH_4$) (Table S6). Reported possible controlling factors of the distribution of calcifiers, foraminifers specifically, are temperature and chlorophyll (as a measure of surface productivity), but also sea-ice cover and therefore, inorganic nutrient availability (Volkmann, 2000; Pados and Spielhagen, 2014; Greco et al., 2019). Several studies found the highest abundances of planktonic foraminifers along the productive sea-ice margins in the Arctic Ocean (Carstens et al., 1997; Volkmann, 2000; Pados and Spielhagen, 2014). These studies were mainly carried out during the late spring or summer months (June-August) and some of them also included the dead (=empty) foraminifers. Our observations of the highest abundances of planktonic foraminifers and pteropods during the summer months (July and August) and at the stations located close to the sea ice edge and in the SIZ in all studied seasons concur well with previous data (Fig. 9a).

The absence (zero abundance) of planktonic foraminifers during winter (March) and the increasing values during spring (May) suggest two possible scenarios: planktonic foraminifers are either seasonally advected from the south by the Atlantic currents and/or during winter they are in a dormant stage resting within the sea ice (as reported by Nigam (2005); Ross and Hallock (2016); Meilland et al. (2022)). The repeatedly higher abundances found at the slope (P6) and basin (P7) stations, influenced by Atlantic currents, combined by the zero abundances found in March, suggest that both processes were at work and followed by their capacity to reproduce rapidly asexually, as observed in the Greenland Sea (Meilland et al., 2022). In the western Barents Sea (Storfjorden) planktonic foraminifers and shelled pteropods were found under ice in late winter (March 2003) (Werner, 2005). We believe therefore, a "nursery" role of the sea ice could exist during winter months for pteropods, but especially for foraminifers. This is the case for other groups such as copepods (Søreide et al., 2010). Specimens of *N. pachyderma* would overwinter as they do in Antarctica (Lipps and Krebs, 1974; Spindler and Dieckmann, 1986) and use a multigenerational strategy combining sexual and asexual reproduction to repopulate the environment successfully within a short time frame (Meilland et al., 2022). Recent laboratory experiments on living individuals of *N. pachyderma* captured from the Greenland Sea documented dormancy and inactivity stages (Westgård et al., 2023).

The low abundances of pteropods together with the smaller sizes in late winter might be due to presence of offspring from the late summer populations. The increasing proportion of larger organisms, as well as their normalized size may be indicative of their life cycle (Fig. 6). The pteropod species *Limacina helicina*, one of the most ubiquitous species in the Arctic, can be found from temperate to polar regions (Bednaršek et al., 2014b; Peck et al., 2016). It is most abundant in the Arctic stations P2–P5 likely following the spring and summer blooms of phytoplankton and zooplankton. *Limacina helicina* is considered an omnivore collecting food using their mucous webs (Lalli and Gilmer, 1989; Gannefors et al., 2005; Conley et al., 2018). At the same time, *L. helicina*, serves as an important food source for larger zooplankton, including the non-shelled pteropod *Clione limacina*, but also for fish, such as polar cod, and sea birds (Gannefors et al., 2005 and references therein). In our study *L. helicina* is most abundant in summer and autumn with large specimens, and less abundant and with juveniles in winter (March) and spring (May) (Fig. 4). The very low abundances found in March agree with the scarce presence (almost zero) reported during pre-spring bloom in a Canadian fjord (Wang et al., 2017). Our observed seasonal pattern is furthermore similar to other studies. In Kongsfjorden, Svalbard, *L. helicina* has a life span of one year, with one or two new generations per year (in spring and summer) (Gannefors et al., 2005). They reach their maximum abundance in late summer and can reach a maximum size of 13 mm (Gannefors et al., 2005; Wang et al., 2017). The highest flux of pteropods in deep sediment traps from the Norwegian Sea (Lofoten Basin at 69° N, Bear Island at 76° N and Fram Strait at 79° N) was recorded in October (Meinecke and Wefer, 1990). Shallow sediment traps from the Fram Strait recorded a rapidly increasing flux of pteropods in summer (July–August) or early autumn (September–October) when it becomes stable until February (Busch et al., 2015). The distribution of shelled pteropods from our study is also associated with temperature, finding higher abundances in colder waters, (Arctic stations P2–P5) (Figs. 4 and S3). In general, they are mainly found in the upper 100 m of the water column (Fig. 4). However, in March we found veliger stages throughout the whole water column (Fig. 4). Their abundances are significantly explained ($p < 0.01$) by a combination of salinity, temperature, and nutrients (NO_3^-), thus showing association with Arctic waters (Table S6).

4.2. Seasonality in carbon standing stocks and export production

Despite the similar absolute abundances of planktonic foraminifers and shelled pteropods in the upper 100 m during summer months (August and July) (Figs. 3 and 4), foraminifers contribute on average 34% to the total (organic and inorganic) export production at 100 m, while pteropods, contributes c. 66% (Table S3).

The carbon standing stocks and export production is well correlated with the seasons. We suggest that the seasonality of carbon standing stocks and export production could be partially associated with the sea-ice edge, the MIZ and SIZ where we find the fresher polar surface water. The calcifiers follow the production of phytoplankton, specially diatoms (Wassmann et al., 1999) and the distribution of zooplankton such as copepods (Falk-Petersen et al., 1999). The highest values of export production recorded along the transect were found in the Arctic stations, P2–P5, where the MIZ was located during all sampling seasons (Figs. 8 and 9). The ice edge, the MIZ and SIZ have been previously described as the most seasonally productive zone for phytoplankton and other organisms that will likely be consumed by foraminifers and pteropods. In particular, the distribution pattern of the foraminifers along the transect in relation to productivity and sea ice distribution is relevant for studies that use foraminifers as proxies to reconstruct past climate and environment. The spatial and temporal variability of foraminifers are also key to better reconstruct past productivity in the fossil record based on the abundance and flux of their shells. In the northern Barents Sea, we have observed the highest foraminiferal export productions in early summer (July, 3.5 ± 3.38 mg $CaCO_3$ m^{-2} d^{-1}) followed by late summer (August, 2.32 ± 1.93 mg $CaCO_3$ m^{-2} d^{-1}) (Table S2). This is later than the peak phytoplankton bloom in the ice-covered northern Barents Sea (Wassmann and Reigstad, 2011), which results in an even more delayed foraminiferal export production (Fig. 8). This late foraminiferal production peak could also be because 2021 was a particularly cold year, keeping a larger (in terms of area) sea-ice cover in the study area and for a longer time than in 2019 (Fig. 1). The Arctic Ocean in general, and our study area in particular, have been reported as extremely variable in degree of sea-ice cover and light availability, resulting in a very strong seasonality and variability of biological production.

The seasonal chlorophyll concentration (=chlorophyll *a*) has been measured at all stations and previously published by Vader (2022). The highest values are found in July, followed by August, and May (Fig. S3). Planktonic foraminifers and pteropods are heterotrophs, feeding on both phytoplankton and smaller zooplankton. We would therefore assume that the higher production of these organisms would occur after the phytoplankton bloom. This has been observed in modelled seasonal distribution of mesozooplankton by Wassmann et al. (2019). However, the production of the calcifiers could be increasing at a slower rate (compared to smaller zooplankton) and their maximum delayed: the July-August maximum may have developed from the spring bloom, while the still high production combined with the larger sizes in December, from a potential late summer phytoplankton bloom. In May and July we observed the highest carbon standing stocks and export productions at the stations closest to the ice edge (P2–P4) and at the time

of maximum spring and early summer phytoplankton productivity (Figs. 7 and 8). Moreover, we need to acknowledge the interannual variability in the Barents Sea region. It is still unclear if years with a higher influence of Atlantic Water (e.g. 2018) could develop a higher production the following year that would hamper the comparison between years. In September 2018 we observed larger carbon standing stocks and export production north of Svalbard (Anglada-Ortiz et al., 2021) than in August and December. We could hypothesize that the carbon standing stock and export production in this region increase until October where it reaches its maximum and subsequently starts decreasing. However, we could also attribute the higher carbon standing stocks from Anglada-Ortiz et al. (2021) to that 2018 was a warmer year than usual, with no ice cover at 82° N in late summer (September) retreating further to 83° N in October (Rasmussen et al., 2018; Husum et al., 2020). In contrast to what we have observed during this seasonal study, in 2018 pteropods were found along the North Svalbard margin in the Arctic Ocean. Given the northward location of the MIZ in late summer 2018, the Arctic zone had spread far north and most likely the production moved along following the retreating sea-ice edge.

5. Conclusions

We identified a clear seasonal pattern in terms of production, size distribution and species abundances and export production of planktonic foraminifers and pteropods, observing the highest values in summer and autumn, and the lowest, in winter (March), as follows:

- In winter (March 2021), with the largest sea-ice extent and with the edge of open and close drift ice located at its southernmost position (76.4° N), is when the lowest abundances of calcifiers were found. The negligible abundance of planktonic foraminifers (<0.4 ind m^{-3}), and the low abundance of pteropods (early veligers) resulted in the lowest carbon standing stock and export production.
- In spring (May 2021) when the sea ice started retreating and where the sea-ice edge between open and close ice drift was located at P2, the abundance of foraminifers and pteropods slowly increased and hence, the carbon standing stock and export production increased compared to late winter. The pteropod community was dominated by both veligers and early veligers, while the planktonic foraminifers, by small and medium sized specimens.
- In summer months, with decreasing sea-ice cover along the transect (P4 very open drift ice in July, and at the edge of open and close drift ice in August) the abundance values reached their highest. The significant abundances of large planktonic foraminifers (>250 μm) and the increased abundance of juvenile pteropods in August 2019 resulted in a higher carbon standing stock and export production compared to July 2021 (they do not differ strongly from the values found in May 2021).
- In late autumn (December 2019), the sea ice covered all stations except the Atlantic station P1 and the southernmost polar station P2, which were at the edge of close and very close ice drift. The abundances in general did not increase, but the relative abundance of adult and juvenile pteropods (>500 μm) did and reached their maximum of all the seasons. In December, we observed the highest normalized size from all the seasons, and hence the highest average carbon standing stock. The average export production was slightly higher than in August.

Furthermore, we found the highest carbon standing stocks and export production of the calcifiers in the seasonal ice zone SIZ (P2–P4) during all seasons closely following the productivity patterns of phytoplankton and other zooplankton. The pteropod community dominates the total carbon standing stock and export production at all seasons, representing on average 83% of both estimates. The foraminiferal distribution pattern was explained by the combination of food availability and temperature and association with Atlantic Water, while the distribution pattern of pteropods was explained by the combination of temperature, salinity, and food availability and association with Arctic Water.

The abundances of marine calcifiers in the northern Barents Sea are expected to change under conditions of "Atlantification" and ocean acidification. The abundances of shelled pteropods will probably decline during years of increased Atlantic inflow, while foraminifers could be increasing. Decreased pH in the water column could result in a lower contribution from pteropods to the carbon standing stocks and export production.

Declaration of Competing Interest

The authors declare that they have no known competing financial interests or personal relationships that could have appeared to influence the work reported in this paper.

Data availability

Data will be published after the acceptance of the paper.

Acknowledgements

We are grateful to the captain and crew from RV *Kronprins Haakon*, cruise participants and cruise leaders (M. Reigstad and T. Gabrielsen; J. Søreide and R. Gradinger; S. Gerland and A. Wold; M. Ludvigsen and P. Assmy; E. Jones and M. Reigstad). We thank the physical oceanographers, L. Marsden, and M. Amargant-Arumí, Y. Bodur and È. Jordà-Molina for the water mass classification, data and *Rstudio* software support. We specially thank N. Espinel-Velasco and V. Pitusi for collecting the samples during the JC 2-1 cruise in July 2021; and K. Zamelczyk who contributed to the study design in 2018, shared the published data and collected the samples for protein measurements during the Q4 cruise in December 2019. We are grateful to M. M. Svenning and A. Didriksen for lending their equipment from the group of Arctic Infection Biology at the Arctic University of Norway, UiT. This study is funded by the Research Council of Norway through the project "The Nansen Legacy" (RCN#276730). This work is contributing to the Spanish Ministry of Science and Innovation, BIOCAL Project (PID2020-113526RB-I00). J.M. is funded through the Cluster of Excellence "The Ocean Floor- Earth's Uncharted Interface" (Receiver unit) of the Deutsche Forschungsgemeinschaft. We thank the four anonymous reviewers for comments and suggestions that greatly helped to improve the manuscript.

Appendix A. Supplementary data

Supplementary data to this article can be found online at https://doi.org/10.1016/j.pocean.2023.103121.

References

Allan, W.H.B., 1960. Ecology of recent planktonic foraminifera: part 2: bathymetric and seasonal distributions in the Sargasso sea off Bermuda. J. Micropaleontol. 6 (4), 373–392. https://doi.org/10.2307/1484218.

Anglada-Ortiz, G., Zamelczyk, K., Meilland, J., Ziveri, P., Chierici, M., Fransson, A., Rasmussen, T.L., 2021. Planktic foraminiferal and pteropod contributions to carbon dynamics in the arctic ocean (North Svalbard Margin). [Original Research]. Front. Mar. Sci. 8 (636) https://doi.org/10.3389/fmars.2021.661158.

Arrigo, K.R., van Dijken, G.L., 2015. Continued increases in Arctic Ocean primary production. Prog. Oceanogr. 136, 60–70.

Bates, N., Mathis, J., 2009. The Arctic Ocean marine carbon cycle: evaluation of air-sea CO 2 exchanges, ocean acidification impacts and potential feedbacks. Biogeosci. 6 (11).

Bednaršek, N., Možina, J., Vogt, M., O'brien, C., Tarling, G.,, 2012a. The global distribution of pteropods and their contribution to carbonate and carbon biomass in the modern ocean. Earth Syst. 4, 167–186.

Bednaršek, N., Tarling, G., Bakker, D., Fielding, S., Jones, E., Venables, H., Ward, P., Kuzirian, A., Lézé, B., Feely, R., 2012b. Extensive dissolution of live pteropods in the Southern Ocean. Nat. Geosci. 5 (12), 881–885.

Bednaršek, N., Tarling, G.A., Bakker, D.C., Fielding, S., Feely, R.A., 2014a. Dissolution dominating calcification process in polar pteropods close to the point of aragonite undersaturation. PLoS One 9 (10), e109183.
Bednaršek, N., Feely, R., Reum, J., Peterson, B., Menkel, J., Alin, S., Hales, B., 2014b. *Limacina helicina* shell dissolution as an indicator of declining habitat suitability owing to ocean acidification in the California Current Ecosystem. Proc. Royal Soc. B 281 (1785), 20140123.
Bednaršek, N., Feely, R.A., Howes, E.L., Hunt, B.P., Kessouri, F., León, P., Lischka, S., Maas, A.E., McLaughlin, K., Nezlin, N.P., 2019. Systematic review and meta-analysis toward synthesis of thresholds of ocean acidification impacts on calcifying pteropods and interactions with warming. Front. Mar. Sci. 6, 227.
Bjørklund, K.R., Kruglikova, S.B., Anderson, O.R., 2012. Modern incursions of tropical Radiolaria into the Arctic Ocean. J. Micropalaeontol. 31 (2), 139–158.
Bluhm, B., Kosobokova, K., Carmack, E., 2015. A tale of two basins: an integrated physical and biological perspective of the deep Arctic Ocean. Prog. Oceanogr. 139, 89–121.
Buitenhuis, E.T., Le Quere, C., Bednaršek, N., Schiebel, R., 2019. Large contribution of pteropods to shallow CaCO3 export. Glob. Biogeochem. Cycles 33 (3), 458–468.
Busch, K., Bauerfeind, E., Nöthig, E.-M., 2015. Pteropod sedimentation patterns in different water depths observed with moored sediment traps over a 4-year period at the LTER station HAUSGARTEN in eastern Fram Strait. Polar Biol. 38, 845–859.
Carstens, J., Hebbeln, D., Wefer, G., 1997. Distribution of planktic foraminifera at the ice margin in the Arctic (Fram Strait). Mar. Micropaleontol. 29 (3–4), 257–269.
Chierici, M., Fransson, A., 2018. Arctic chemical oceanography at the edge: focus on carbonate chemistry (chapter 13). In: Wassmann, P. (Ed.), At the edge.
Chierici, M., Jones, E., Lødemel, H.H., 2021a. Water column data on dissolved inorganic nutrients (nitrite, nitrate, phosphate and silicic acid) from the Nansen LEGACY joint cruise KH 2019706 with R.V. Kronprins Haakon, 5-27 August 2019. 10.21335/NMDC-1472517325.
Chierici, M., Jones, E., Lødemel, H.H., 2021b. Water column data on dissolved inorganic nutrients (nitrite, nitrate, phosphate and silicic acid) from the Nansen LEGACY seasonal cruise Q4, KH 2019711 with R.V. Kronprins Haakon. 10.21335/NMDC-1629206101.
Conley, K.R., Lombard, F., Sutherland, K.R., 2018. Mammoth grazers on the ocean's minuteness: a review of selective feeding using mucous meshes. Proc. R. Soc. B Biol. Sci. 285 (1878), 20180056.
Dalpadado, P., Arrigo, K.R., Hjøllo, S.S., Rey, F., Ingvaldsen, R.B., Sperfeld, E., van Dijken, G.L., Stige, L.C., Olsen, A., Ottersen, G., 2014. Productivity in the Barents Sea - response to recent climate variability. PLoS One 9 (5), e95273. https://doi.org/10.1371/journal.pone.0095273.
Descamps, S., Aars, J., Fuglei, E., Kovacs, K.M., Lydersen, C., Pavlova, O., Pedersen, Å.Ø., Ravolainen, V., Strøm, H., 2017. Climate change impacts on wildlife in a High Arctic archipelago–Svalbard, Norway. Glob. Change Biol. 23 (2), 490–502.
Fabry, V.J., 2008. Marine calcifiers in a high-CO2 ocean. Science 320 (5879), 1020–1022.
Falk-Petersen, S., Pedersen, G., Kwasniewski, S., Hegseth, E.N., Hop, H., 1999. Spatial distribution and life-cycle timing of zooplankton in the marginal ice zone of the Barents Sea during the summer melt season in 1995. J. Plankton Res. 21 (7).
Feely, R.A., Sabine, C.L., Lee, K., Berelson, W., Kleypas, J., Fabry, V.J., Millero, F.J., 2004. Impact of anthropogenic CO2 on the CaCO3 system in the oceans. Science 305 (5682), 362–366.
Fer, I., Peterson, A.K., Nilsen, F., 2022. Atlantic water boundary current along the southern Yermak Plateau, Arctic Ocean. J. Geophys. Res. Oceans e2023JC019645.
Fetterer, F., K. Knowles, W. N. Meier, M. Savoie, A. K. Windnagel., 2017. Sea Ice Index, Version 3 [Data Set]. Boulder, Colorado USA. National Snow and Ice Data Center.
Gannefors, C., Böer, M., Kattner, G., Graeve, M., Eiane, K., Gulliksen, B., Hop, H., Falk-Petersen, S., 2005. The Arctic sea butterfly *Limacina helicina*: lipids and life strategy. Mar. Biol. 147 (1), 169–177.
Gerland, S., 2022. CTD data from Nansen Legacy Cruise - Seasonal cruise Q1. 10.21335/NMDC-1491279668.
Greco, M., Jonkers, L., Kretschmer, K., Bijma, J., Kucera, M., 2019. Depth habitat of the planktonic foraminifera *Neogloboquadrina pachyderma* in the northern high latitudes explained by sea-ice and chlorophyll concentrations. Biogeosciences 16 (17), 3425–3437.
Greco, M., Werner, K., Zamelczyk, K., Rasmussen, T.L., Kucera, M., 2022. Decadal trend of plankton community change and habitat shoaling in the Arctic gateway recorded by planktonic foraminifera. Glob. Chang. Biol. 28 (5), 1798–1808.
Hemleben, C., Spindler, M., Anderson, O.R., 1989. Modern Planktonic Foraminifera. Springer-Verlag Neew York Inc. 10.1007/978-1-4612-3544-6.
Hunt, B.P.V., Pakhomov, E.A., Hosie, G.W., Siegel, V., Ward, P., Bernard, K., 2008. Pteropods in Southern Ocean ecosystems. Prog. Oceanogr. 78 (3), 193–221. https://doi.org/10.1016/j.pocean.2008.06.001.
Husum, K., Ninnemann, U., Rydningen, T.A., Alve, E., El Bani Altuna, N., Braaten, A.H., Eilertsen, V., Gamboa, V., Kjøller, M.R., Orme, L., Rutledal, S., Tessin, A., Zindorf, M., 2020. Paleo Cruise 2018: Cruise Report. The Nansen Legacy Report Series 3/2020.
Jacobs, J., Barry, R., Weaver, R., 1975. Fast ice characteristics, with special reference to the eastern Canadian Arctic. Polar Rec. 17(110), 521–536. 10.1017/S0032247400032484.
Jones, E., Chierici, M., Lødemel, H.H., Møgster, J., Fonnes, L.L., 2022a. Water column data on dissolved inorganic nutrients (nitrite, nitrate, phosphate and silicic acid) from Process (P) stations during the Nansen LEGACY joint cruise JC2-1, 2021708, with R.V. Kronprins Haakon, 14-24 July 2021. 10.21335/NMDC-1747434716.
Jones, E., Chierici, M., Lødemel, H.H., Møgster, J., Fonnes, L.L., 2022b. Water column data on dissolved inorganic nutrients (nitrite, nitrate, phosphate and silicic acid) from Process (P) stations during the Nansen LEGACY seasonal cruise Q1, 2021703, with R.V. Kronprins Haakon, 4-17 March 2021. 10.21335/NMDC-762320451.
Jones, E., Chierici, M., Lødemel, H.H., Møgster, J., Fonnes, L.L., 2022c. Water column data on dissolved inorganic nutrients (nitrite, nitrate, phosphate and silicic acid) from Process (P) stations during the Nansen LEGACY seasonal cruise Q2, 2021704, with R.V. Kronprins Haakon, 30 April–18 May 2021. 10.21335/NMDC-487023368.
Jones, E., Chierici, M., Fransson, A., Assman, K., Renner, A.H.H., Lødemel, H.H. (this issue). Inorganic carbon and nutrient dynamics in the marginal ice zone of the Barents Sea: seasonality and implications for ocean acidification.
Jones, E., 2022. CTD data from Nansen Legacy Cruise - Joint cruise 2-1. 10.21335/NMDC-2085836005.
Jonkers, L., Kučera, M., 2015. Global analysis of seasonality in the shell flux of extant planktonic Foraminifera. Biogeosciences 12 (7), 2207–2226.
Kinnard, C., Zdanowicz, C.M., Koerner, R.M., Fisher, D.A., 2008. A changing Arctic seasonal ice zone: Observations from 1870–2003 and possible oceanographic consequences. Geophys. Res. Lett. 35 (2).
Lalli, C.M., Gilmer, R.W., 1989. Pelagic Snails: The Biology of Holoplanktonic Gastropod Mollusks. Stanford University Press.
Langer, M.R., 2008. Assessing the contribution of foraminiferan protists to global ocean carbonate production 1. J. Eukaryot. Microbiol. 55 (3), 163–169.
Lee, Y.J., Matrai, P.A., Friedrichs, M.A., Saba, V.S., Antoine, D., Ardyna, M., Asanuma, I., Babin, M., Bélanger, S., Benoît-Gagné, M., 2015. An assessment of phytoplankton primary productivity in the Arctic Ocean from satellite ocean color/in situ chlorophyll-a based models. J. Geophys. Res. Oceans 120 (9), 6508–6541.
Lipps, J.H., Krebs, W.N., 1974. Planktonic foraminifera associated with Antarctic sea ice. J. Foramin. Res. 4 (2), 80–85.
Loeng, H., 1991. Features of the physical oceanographic conditions of the Barents Sea. Polar Res. 10 (1), 5–18.
Ludvigsen, M., 2022. CTD data from Nansen Legacy Cruise - Seasonal cruise Q2. 10.21335/NMDC-515075317.
Lundesgaard, Ø., Sundfjord, A., Lind, S., Nilsen, F., Renner, A.H.H., 2022. Import of Atlantic Water and sea ice controls the ocean environment in the northern Barents Sea. Ocean Sci. 18 (5), 1389–1418. https://doi.org/10.5194/os-18-1389-2022.
Manno, C., Bednaršek, N., Tarling, G.A., Peck, V.L., Comeau, S., Adhikari, D., Bakker, D. C., Bauerfeind, E., Bergan, A.J., Berning, M.I., 2017. Shelled pteropods in peril: assessing vulnerability in a high CO2 ocean. Earth Sci. Rev. 169, 132–145.
Manno, C., Morata, N., Primicerio, R., 2012. *Limacina retroversa*'s response to combined effects of ocean acidification and sea water freshening. Estuar. Coast. Shelf Sci. 113, 163–171.
Manno, C., Pavlov, A., 2013. Living planktonic foraminifera in the Fram Strait (Arctic): absence of diel vertical migration during the midnight sun. Hydrobiologia 721 (1), 285–295.
Meilland, J., Howa, H., Monaco, C.L., Schiebel, R., 2016. Individual planktic foraminifer protein-biomass affected by trophic conditions in the Southwest Indian Ocean, 30° S–60° S. Mar. Micropaleontol. 124, 63–74.
Meilland, J., Schiebel, R., Monaco, C.L., Sanchez, S., Howa, H., 2018. Abundances and test weights of living planktic foraminifers across the Southwest Indian Ocean: Implications for carbon fluxes. Deep Sea Res. Part I 131, 27–40.
Meilland, J., Howa, H., Hulot, V., Demangel, I., Salaun, J., Garlan, T., 2020. Population dynamics of modern planktonic foraminifera in the western Barents Sea. Biogeosciences 17 (6), 1437–1450.
Meilland, J., Ezat, M.M., Westgård, A., Manno, C., Morard, R., Siccha, M., Kucera, M., 2022. Rare but persistent asexual reproduction explains the success of planktonic foraminifera in polar oceans. J. Plankton Res. 1–18 https://doi.org/10.1093/plankt/fbac069.
Meinecke, G., Wefer, G., 1990. Seasonal pteropod sedimentation in the Norwegian Sea. Palaeogeogr. Palaeoclimatol. Palaeoecol. 79 (1), 129–147. https://doi.org/10.1016/0031-0182(90)90109-K.
Moy, A.D., Howard, W.R., Bray, S.G., Trull, T.W., 2009. Reduced calcification in modern Southern Ocean planktonic foraminifera. Nat. Geosci. 2 (4), 276–280.
Nigam, R., 2005. Sediment traps as a new tool for estimation of longevity of planktonic foraminifera.
Norwegian Meteorological Institute Ice service, 2022. https://cryo.met.no/en/ice-service.
Ofstad, S., Meilland, J., Zamelczyk, K., Chierici, M., Fransson, A., Gründger, F., Rasmussen, T.L., 2020. Development, productivity, and seasonality of living planktonic foraminiferal faunas and *Limacina helicina* in an Area of intense methane seepage in the Barents Sea. J. Geophys. Res. Biogeosci. 125(2), e2019JG005387.
Orr, J.C., Fabry, V.J., Aumont, O., Bopp, L., Doney, S.C., Feely, R.A., Gnanadesikan, A., Gruber, N., Ishida, A., Joos, F., 2005. Anthropogenic ocean acidification over the twenty-first century and its impact on calcifying organisms. Nature 437 (7059), 681–686.
Pados, T., Spielhagen, R.F., 2014. Species distribution and depth habitat of recent planktic foraminifera in Fram Strait. Arctic Ocean. Polar Res. 33 (1), 22483.
Peck, V.L., Tarling, G.A., Manno, C., Harper, E.M., Tynan, E., 2016. Outer organic layer and internal repair mechanism protects pteropod *Limacina helicina* from ocean acidification. Deep Sea Res., Part IITopical Studies in Oceanography 127, 41–52. https://doi.org/10.1016/j.dsr2.2015.12.005.
Peck, V.L., Oakes, R.L., Harper, E.M., Manno, C., Tarling, G.A., 2018. Pteropods counter mechanical damage and dissolution through extensive shell repair. Nat. Commun. 9 (1), 1–7.
Pieńkowski, A.J., Husum, K., Belt, S.T., Ninnemann, U., Köseoğlu, D., Divine, D.V., Smik, L., Knies, J., Hogan, K., Noormets, R., 2021. Seasonal sea ice persisted through the Holocene Thermal Maximum at 80°N. Commun. Earth Environ. 2 (1), 124. https://doi.org/10.1038/s43247-021-00191-x.

Polyakov, I.V., Alkire, M.B., Bluhm, B.A., Brown, K.A., Carmack, E.C., Chierici, M., Danielson, S.L., Ellingsen, I., Ershova, E.A., Gårdfeldt, K., 2020. Borealization of the Arctic Ocean in response to anomalous advection from sub-Arctic seas. Front. Mar. Sci. 7, 491.

Rasmussen, T.L., Laberg, J.S., Ofstad, S., Rydningen, T.A., Åström, E., El Bani Altuna, N., Lasabuda, A., Carrol, M., 2018. Cruise Report: AMGG Cruise to the Northern and Eastern Svalbard Margin, Department of Geosciences, UiT, Arctic University of Norway, N-9037. Tromsø, Norway.

Reigstad, M., Wassmann, P., Riser, C.W., Øygarden, S., Rey, F., 2002. Variations in hydrography, nutrients and chlorophyll a in the marginal ice-zone and the central Barents Sea. J. Mar. Syst. 38 (1–2), 9–29.

Reigstad, M., 2022. CTD data from Nansen Legacy Cruise - Seasonal cruise Q3. 10.21335/NMDC-1107597377.

Ross, B.J., Hallock, P., 2016. Dormancy in the foraminifera: a review. J. Foramin. Res. 46 (4), 358–368.

Saher, M., Kristensen, D.K., Hald, M., Pavlova, O., Jørgensen, L.L., 2012. Changes in distribution of calcareous benthic foraminifera in the central Barents Sea between the periods 1965–1992 and 2005–2006. Glob. Planet. Change 98–99, 81–96. https://doi.org/10.1016/j.gloplacha.2012.08.006.

Sakshaug, E., 1997. Biomass and productivity distributions and their variability in the Barents Sea. ICES Mar. Sci. Symp. 54 (3), 341–350.

Sakshaug, E., Skjoldal, H.R., 1989. Life at the ice edge. Ambio (Sweden).

Sakshaug, E., Slagstad, D., 1991. Sea ice and wind: effects on primary productivity in the Barents Sea. Atmos.-Ocean 30 (4), 579–591.

Schiebel, R., 2002. Planktic foraminiferal sedimentation and the marine calcite budget. Glob. Biogeochem. Cycles 16 (4), 3-1-3-21.

Schiebel, R., Hemleben, C., 2000. Interannual variability of planktic foraminiferal populations and test flux in the eastern North Atlantic Ocean (JGOFS). Deep-Sea Res. II: Top. Stud. Oceanogr. 47(9-11), 1809–1852.

Schiebel, R., Movellan, A., 2012. First-order estimate of the planktic foraminifer biomass in the modern ocean. Earth Syst. Sci. Data 4, 75–89.

Schneider, C.A., Rasband, W.S., Eliceiri, K.W., 2012. NIH Image to ImageJ: 25 years of image analysis. Nat. Methods 9 (7), 671–675.

Smedsrud, L.H., Muilwijk, M., Brakstad, A., Madonna, E., Lauvset, S.K., Spensberger, C., Born, A., Eldevik, T., Drange, H., Jeansson, E., 2022. Nordic Seas heat loss, Atlantic inflow, and Arctic sea ice cover over the last century. Rev. Geophys. 60(1), e2020RG000725.

Søreide, J.E., Leu, E.V., Berge, J., Graeve, M., Falk-Petersen, S., 2010. Timing of blooms, algal food quality and *Calanus glacialis* reproduction and growth in a changing Arctic. Glob. Chang. Biol. 16 (11), 3154–3163.

Søreide, J.E., 2022. CTD data from Nansen Legacy Cruise - Seasonal cruise Q4. 10.21335/NMDC-301551919.

Spindler, M., Dieckmann, G.S., 1986. Distribution and abundance of the planktic foraminifer Neogloboquadrina pachyderma in sea ice of the Weddell Sea (Antarctica). Polar Biol. 5 (3), 185–191.

Stangeew, E., 2001. Distribution and Isotopic Composition of Living Planktonic Foraminifera *N. pachyderma* (sinistral) and *T. quinqueloba* in the High Latitude North Atlantic. Christian-Albrechts Universität Kiel.

Steinsund, P., 1994. Benthic Foraminifera in Surface Sediments of the Barents and Kara Seas: Modern and Late Quaternary Applications. University of Tromsø, Tromsø, 111 pp.

Subhas, A.V., Dong, S., Naviaux, J.D., Rollins, N.E., Ziveri, P., Gray, W., Rae, J.W., Liu, X., Byrne, R.H., Chen, S., 2022. Shallow calcium carbonate cycling in the North Pacific Ocean. Glob. Biogeochem. Cycles e2022GB007388.

Sundfjord, A., Assmann, K.M., Lundesgaard, Ø., Renner, A.H.H., Lind, S., Ingvaldsen, R. B., 2020. Suggested water mass definitions for the central and northern Barents Sea, and the adjacent Nansen Basin: Workshop Report. (2703-7525). The Nansen Legacy Report Series 8/2020. 10.7557/nlrs.5707.

Tell, F., Jonkers, L., Meilland, J., Kucera, M., 2022. Upper-ocean flux of biogenic calcite produced by the Arctic planktonic foraminifera *Neogloboquadrina pachyderma*. Biogeosciences 19 (20), 4903–4927. https://doi.org/10.5194/bg-19-4903-2022.

Vader, A., 2022. Chlorophyll A and phaeopigments Nansen. Legacy. https://doi.org/10.21335/NMDC-1371694848.

Vernet, M., Ellingsen, I.H., Seuthe, L., Slagstad, D., Cape, M.R., Matrai, P.A., 2019. Influence of phytoplankton advection on the productivity along the Atlantic water inflow to the Arctic Ocean [Original Research]. Front. Mar. Sci. 6 (583) https://doi.org/10.3389/fmars.2019.00583.

Vihtakari., M., 2020. PlotSvalbard: PlotSvalbard - Plot research data from Svalbard on maps. Version R package version (9), 2. https://github.com/MikkoVihtakari/PlotSvalbard.

Volkmann, R., 2000. Planktic foraminifers in the outer Laptev Sea and the Fram Strait—Modern distribution and ecology. J. Foramin. Res. 30 (3), 157–176.

Wadhams, P., 1986. The Seasonal Ice Zone. In: Untersteiner, N. (Ed.), The Geophysics of Sea Ice. Springer, US, pp. 825-991. 10.1007/978-1-4899-5352-0_15.

Wang, K., Hunt, B.P., Liang, C., Pauly, D., Pakhomov, E.A., 2017. Reassessment of the life cycle of the pteropod *Limacina helicina* from a high resolution interannual time series in the temperate North Pacific. ICES Mar. Sci. 74 (7), 1906–1920.

Wassmann, P., Ratkova, T., Andreassen, I., Vernet, M., Pedersen, G., Rey, F., 1999. Spring bloom development in the marginal ice zone and the central Barents Sea. Mar. Ecol. 20 (3–4), 321–346.

Wassmann, P., Reigstad, M., 2011. Future Arctic Ocean seasonal ice zones and implications for pelagic-benthic coupling. Oceanography 24 (3), 220–231.

Wassmann, P., Slagstad, D., Ellingsen, I., 2019. Advection of mesozooplankton into the Northern Svalbard shelf region [original research]. Front. Mar. Sci. 6 (458) https://doi.org/10.3389/fmars.2019.00458.

Werner, I., 2005. Living conditions, abundance and biomass of under-ice fauna in the Storfjord area (western Barents Sea, Arctic) in late winter (March 2003). Polar Biol. 28 (4), 311–318.

Westgård, A., Ezat, M.M., Chalk, T.B., Chierici, M., Foster, G.L., Meilland, J., 2023. Large-scale culturing of *Neogloboquadrina pachyderma*, its growth in, and tolerance of, variable environmental conditions. J. Plankton Res.

Zamelczyk, K., Fransson, A., Chierici, M., Jones, E., Meilland, J., Anglada-Ortiz, G., Lødemel, H.H., 2021. Distribution and abundances of planktic foraminifera and shelled pteropods during the polar night in the sea-ice covered northern Barents Sea. Front Mar. Sci. 1516.

Ziveri, P., de Bernardi, B., Baumann, K.-H., Stoll, H.M., Mortyn, P.G., 2007. Sinking of coccolith carbonate and potential contribution to organic carbon ballasting in the deep ocean. Deep Sea Res. Part II 54 (5–7), 659–675.

Ziveri, P., Gray, W.R., Anglada-Ortiz, G., Manno, C., Grelaud, M., Incarbona, A., Rae, J. W.B., Subhas, A.V., Pallacks, S., White, A., Adkins, J.F., Berelson, W., 2023. Pelagic calcium carbonate production and shallow dissolution in the North Pacific Ocean. Nat. Commun. 14 (1), 805.